# Conservation paleobiology on Minami-Daito Island, Okinawa, Japan: Anthropogenic extinction of cave-dwelling bats on a tropical oceanic island

Yuri Kimura [Corresp., 1, 2] , Dai Fukui [3] , Mizuko Yoshiyuki [4] , Kazuaki Higashi [5]

[1] Department of Geology and Paleontology, National Museum of Nature and Science, Tsukuba, Ibaraki, Japan

[2] Institut Català de Paleontologia Miquel Crusafont, ICTA-ICP, Barcelona, Spain

[3] The University of Tokyo Hokkaido Forest, Graduate School of Agricultural and Life Sciences, The University of Tokyo, Furano, Hokkaido, Japan

[4] Department of Agriculture, Tokyo University of Agriculture, Atsugi, Kanagawa, Japan

[5] Office Key Point, Minami-Daito, Okinawa, Japan

Corresponding Author: Yuri Kimura
Email address: ykimura@kahaku.go.jp

**Background**. With strong environmental and geographic filtration, vertebrates incapable of flying and swimming are often extirpated from island ecosystems. Minami-Daito Island is an oceanic island in Okinawa, Japan that harbors the Daito flying fox (*Pteropus dasymallus daitoensis*), a subspecies of the fruit bat and the only extant mammal endemic to the island. However, the skeleton of a cave-dwelling bat *Rhinolophus* sp. and fossil guano were briefly reported in a previous study.

**Methods**. Here, we present evidence for the anthropogenic extirpation of two species of cave-dwelling bats (*Miniopterus* sp. & *Rhinolophus* sp.) from Minami-Daito Island. Our goal is to reliably constrain the ages of the extirpated bat species by a multiproxy approach. Because skeletal materials did not preserve sufficient bone collagen for direct radiocarbon dating, we alternatively examined guano-like deposits based on SEM observation and Fourier-transform infrared spectroscopy (FTIR) along with stable carbon and nitrogen isotope analyses for possible indirect dating. We also examined stable carbon isotopes in bone apatite, assuming that an isotopic signal of $C_4$ plants on the bat bones links to sugarcane plantation on the island based on the historical knowledge that early human settlers quickly replaced the island's native $C_3$ forests with sugarcane ($C_4$ perennial grass) plantation from 1900 onward.

**Results**. Our cave survey documents the remains of *Miniopterus* sp. from the island for the first time. Based on the unique taphonomic conditions (unpermineralized bones, disarticulated skeletons closely scattered without sediment cover, various degrees of calcite crystal growth around bones) and a radiocarbon age of a humic sample, we suggest that the maximum age constraint of *Miniopterus* sp. and *Rhinolophus* sp. is 4,640 calBP. Based on a series of analyses, we conclude that the guano-like deposits are composed not of bat guano but mainly of humic substances; however, a hydroxyapatite crust associated with bat-lying stalagmites may be derived from bat feces. Stable carbon isotope analysis of bone apatite revealed $C_4$ signals in various degrees, confirming that small populations of cave-dwelling bats persisted on Minami-Daito Island after 1900.

**Conclusions**. The results of this study indicate that these populations remained rather small and did not leave many generations and that the estimated ages can be bracketed from 4,640 calBP to the post-1900 (perhaps, until the 1950s). They likely faced a continuously high mortality risk due to severe anthropogenic stresses on the island, where most of the forests were turned into sugarcane plantations within a few decades in the early 20th century. A result of hearing surveys to local residents suggests the

latest remnants most likely disappeared on the island concurrently with the introduction of chemical pesticides after World War II.

3    Conservation paleobiology on Minami-Daito Island, Okinawa, Japan: Anthropogenic extinction

4    of cave-dwelling bats on a tropical oceanic island

9    Yuri Kimura[1,2*], Dai Fukui[3], Mizuko Yoshiyuki[4], Kazuaki Higashi[5]

12    Yuri Kimura https://orcid.org/0000-0002-7621-9901
13    Dai Fukui https://orcid.org/0000-0002-5449-4283

16    [1] Department of Geology and Paleontology, National Museum of Nature and Science, 4-1-1

17    Amakubo, Tsukuba, Ibaraki, 305-0005, Japan; e-mail: ykimura.research@gmail.com.

20    [2] Institut Català de Paleontologia Miquel Crusafont, ICTA-ICP. Edifici Z. Carrer de les

21    Columnes, s/n., Campus de la Universitat Autònoma de Barcelona. E-08193 Cerdanyola del

22    Vallès, Barcelona, Spain

24    [3] The University of Tokyo Hokkaido Forest, Graduate School of Agricultural and Life Sciences,

25    The University of Tokyo, 9-61, Yamabe-Higashimachi, Furano, Hokkaido 079-1563, Japan

27    [4] Department of Agriculture, Tokyo University of Agriculture, 1737 Funako, Atsugi, Kanagawa

28    243-0034, Japan

30    5 Office Key Point, Minami-Daito Island, Okinawa

35   **Keywords**

36   Anthropogenic extinction; extirpation; Chiroptera; Mammalia; Conservation paleobiology;

37   Zoology; stable carbon isotopes; FTIR; fossil guano

41   **Abstract**

43   **Background**. With strong environmental and geographic filtration, vertebrates incapable of

44   flying and swimming are often extirpated from island ecosystems. Minami-Daito Island is an

45   oceanic island in Okinawa, Japan that harbors the Daito flying fox (*Pteropus dasymallus*

46   *daitoensis*), a subspecies of the fruit bat and the only extant mammal endemic to the island.

47   However, the skeleton of a cave-dwelling bat *Rhinolophus* sp. and fossil guano were briefly

48   reported in a previous study.

49   **Methods**. Here, we present evidence for the anthropogenic extirpation of two species of cave-

50   dwelling bats (*Miniopterus* sp. & *Rhinolophus* sp.) from Minami-Daito Island. Our goal is to

51   reliably constrain the ages of the extirpated bat species by a multiproxy approach. Because

52   skeletal materials did not preserve sufficient bone collagen for direct radiocarbon dating, we

53   alternatively examined guano-like deposits based on SEM observation and Fourier-transform

54   infrared spectroscopy (FTIR) along with stable carbon and nitrogen isotope analyses for possible

55   indirect dating. We also examined stable carbon isotopes in bone apatite, assuming that an

56   isotopic signal of $C_4$ plants on the bat bones links to sugarcane plantation on the island based on

57   the historical knowledge that early human settlers quickly replaced the island's native $C_3$ forests

58   with sugarcane ($C_4$ perennial grass) plantation from 1900 onward.

59   **Results**. Our cave survey documents the remains of *Miniopterus* sp. from the island for the first

60   time. Based on the unique taphonomic conditions (unpermineralized bones, disarticulated

61   skeletons closely scattered without sediment cover, various degrees of calcite crystal growth

62   around bones) and a radiocarbon age of a humic sample, we suggest that the maximum age

63   constraint of *Miniopterus* sp. and *Rhinolophus* sp. is 4,640 calBP. Based on a series of analyses,

64   we conclude that the guano-like deposits are composed not of bat guano but mainly of humic

65   substances; however, a hydroxyapatite crust associated with bat-lying stalagmites may be

66   derived from bat feces. Stable carbon isotope analysis of bone apatite revealed $C_4$ signals in

67   various degrees, confirming that small populations of cave-dwelling bats persisted on Minami-

68   Daito Island after 1900.

69   **Conclusions**. The results of this study indicate that these populations remained rather small and

70   did not leave many generations and that the estimated ages can be bracketed from 4,640 calBP to

71   the post-1900 (perhaps, until the 1950s). They likely faced a continuously high mortality risk due

72   to severe anthropogenic stresses on the island, where most of the forests were turned into

73   sugarcane plantations within a few decades in the early 20th century. A result of hearing surveys

74   to local residents suggests the latest remnants most likely disappeared on the island concurrently

75   with the introduction of chemical pesticides after World War II.

76

77

78

79

80  **Introduction**

81

82      Insular systems such as remote islands, volcanic lakes, and deep caves, have offered

83  natural testing grounds for understanding how migration, speciation, and extinction function in

84  the long-term ecological dynamics of life (van der Geer et al., 2010). Generally, vertebrate

85  animals capable of flying, swimming, or more passively rafting in water compose native faunas

86  in these systems, and geographic barriers and environmental filters yield species-poor

87  communities with a high percentage of endemic taxa (e.g., Albert et al., 2017; van der Geer et

88  al., 2010). In these settings, human colonization has increased extinction risks of native species

89  by economic activities and bringing introduced species in the natural ecosystem. Thus, long-term

90  monitoring and quantification of species richness and biodiversity on these islands have gained

91  recent attention regarding conservation against further anthropogenic extinction (e.g., Allentoft a

92  et al., 2014; Wood et al., 2017; Carpenter et al., 2020).

93      The Daito Islands in Japan are an archipelago of oceanic islands that have been separated

94  from the closest landmass since their emergence. Historically, these islands were uninhabited by

95  humans until the first exploitation over 120 years ago in 1899-1900. Prior to the arrival of

96  humans, dense native forests comprising subtropical fan palm trees (*Livistona chinensis* var.

97  *amanoi*), *Neolitsea sericea* var. *argentea,* banyans, and the evergreen shrub (*Excoecaria*

98  *formosana* var. *daitoinsularis*) harbored endemic species of birds, insects, and fruit bats. By the

99  1930s, the rapid development of sugarcane plantation along with the filling of underground caves

100  and sinkholes for land improvement and military construction caused severe and irreversible

101  changes in vegetation (Editorial Committee of the History of Minami-Daito Village, 1990). At

102   present, any remaining natural forests are limited to the rims of the islands (Fig. 1A; Google

103   Earth, 2021). Under a combination of high anthropogenic stresses and biogeographical

104   constraints, the Daito flying fox (*Pteropus dasymallus daitoensis*), a subspecies of the Ryukyu

105   flying fox (*Pteropus dasymallus*), is the only extant mammal species endemic to the Daito

106   Islands.

107        Although the endangered Daito flying fox is the only native mammal on the Daito Islands

108   today, Shimojana (1978) reported a skeleton of a cave-dwelling bat species found in Hoshino

109   Cave, the only tourist cave on Minami-Daito Island, and classified the skeleton as *Rhinolophus*

110   sp. Shimojana (1978) also noted that large amounts of fossil bat guano were present in the cave.

111   Cave-dwelling bats, including fossils and extant ones, have not been documented on the island

112   since then. Recently, based on information about additional skeletons of insectivorous bats in a

113   different cave on the same island, we collected skeletal remains that belong to two bat species of

114   different sizes.

115        In this study, we aim to constrain the ages of the extirpated bat species using a

116   multiproxy approach. Unfortunately, bone collagen was not preserved in the collected bat bones

117   (details in the Materials and Methods section), which makes direct radiocarbon dating

118   impossible. Alternatively, for indirect radiocarbon dating, we examined (1) the guano-like

119   deposits based on SEM observation and Fourier-transform infrared spectroscopy (FTIR) along

120   with stable carbon and nitrogen isotope analyses to test the hypothesis that the "guano deposits"

121   observed by Shimojana (1978) are truly fossil bat guano and (2) conduct stable carbon isotope

122   analysis in bone apatite of the bats to detect a signal of $C_4$ plants. Stable carbon isotopes in bone

123   apatite reflect consumed diet of the bats and are not directly related to age determination. For age

124   constraints of the extirpated bats, we take advantage of the historical fact that the island's native

125    $C_3$ forests were quickly deforested and replaced with sugarcane ($C_4$ perennial grass) plantation

126    from the first development by early human settlers from 1900 onward (details in the Materials

127    and Methods section). It is assumed here that a signal of $C_4$ plants in the bat bones was caused by

128    the presence of sugarcane plantation on the island and thus that the bat individuals were alive

129    after 1900. We further discuss that the extirpation of the cave-dwelling bats was probably caused

130    by high anthropogenic stresses on the small island.

131

132

133

134

135   **Geological Setting**

136

137        The Daito Islands are oceanic islands located on the Philippine Sea Plate, nearly 400 km

138   southeast of Okinawa Island in Okinawa Prefecture, Japan, comprising Minami-Daito Island

139   (*Minamidaitōjima*, 30.74 km²), Kita-Daito Island (*Kitadaitōjima*, 12.71 km²), and Oki-Daito

140   Island (*Okidaitōjima*, 1.19km²), listed in order of decreasing surface area (Fig. 1A-B; Editorial

141   Committee of the History of Minami-Daito Village, 1990). Oki-Daito Island is uninhabitable

142   because of decades of firing exercises by the United States Navy, so ecological studies have only

143   been conducted on Minami-Daito Island and Kita-Daito Island. The Daito Islands are atolls that

144   drifted to its current position from near the equator where coral reefs began to accumulate over

145   50 million years ago (Klein and Kobayashi, 1980; Seno and Maruyama, 1984) and were uplifted

146   during the Pliocene and Pleistocene epochs on the forebulge of the Philippine Sea Plate prior to

147   subduction along the Ryukyu Trench (Ohde and Elderfield, 1992). Based on samples from

148   boring surveys on Kita-Daito Island between 1934 to 1936, the carbonate deposits on the islands

149   are up to 430m thick, and the oldest strata are early Miocene in age (Ohde and Elderfield, 1992).

150        On Minami-Daito Island, Urushibara-Yoshino (2012) recognized two informal

151   lithostratigraphic units of dolomitized limestone on the island, including the "Lower Daito

152   Layer" and the more fossiliferous "Upper Daito Layer," which are separated by an unconformity

153   that was interpreted as the surface of karstification. Differential erosional rates of the dolomitized

154   limestone layers have formed the unique topography of Minami-Daito Island that is

155   characterized by basin-shaped lowlands ("Hagu Shita" in local vernacular) of the heavily

156   karstified Lower Daito Layer surrounded by topographic highlands ("Hagu Ue" in local

157   vernacular) of the Upper Daito Layer averaging 40m above sea level that form rims along the

158   coast (Urushibara-Yoshino, 2012; Nambu, 2003). A coastal bench ~10m above sea level is

159    overlain by a thin coral limestone dated to ~125 ka, corresponding to the Marine Isotope Stage

160    5e during the last interglacial period in the Pleistocene (Ota et al., 1991), whereas the lowest

161    coastal bench at ~3m above sea level may have formed more recently during a mid-Holocene

162    sea-level highstand, the age of which is 6,500-5,000 BP (Umitsu, 1991 for ages; Urushibara-

163    Yoshino, 2012).

164

165

166

167

168     **Materials and Methods**

169

170

171     **Skeletal remains in the caves of Minami-Daito Island**

172     There are countless sinkholes (dolines) and caves on Minami-Daito Island, some of

173     which preserve the remains of extirpated bats. We collected vertebrate skeletal remains and bat

174     guano-like deposits from two of these caves, which are a public cave called Hoshino Cave (also

175     called *Hoshinodō* or Hoshinodo Cave, as "*dō*" means "cave" in Japanese) and a privately-owned

176     cave informally called "Cave A" (Fig. 1A). Fieldwork was conducted in January 2016 and

177     January 2018 because the $CO_2$ concentration levels in the caves are lowest during the winter. All

178     fieldwork was conducted outside national parks or restricted areas designated by the Nature

179     Conservation Act.

180     Cave A is accessible via several spots where the ceiling has collapsed, but we entered

181     through the main natural entrance, which is located in the Hagu Shita basin near the basin-side

182     edge of the Hagu Ue rim (Fig. 1C). Because there is no published map for Cave A, we made a

183     simple route map from the main entrance to our sample locations (Fig. 1D). Skeletal remains of

184     insectivorous bats were collected from a small hall about 60 m north of the main entrance.

185     Generally, skeletal remains are scattered, suggesting that these individuals were not transported

186     by water flow (Fig. 2A–B). In Cave A, we observed that at least four individuals were almost

187     completely articulated and embedded by thin crusts of flowstone, which have served as

188     protection against dissociation and bone decay (Fig. 3). Two of these individuals were collected

189     (Fig. 2D). For others, bones are disarticulated and selectively preserved with a bias toward long

190     bones (radius, metacarpal, etc.), tympanic bullae, and jaws. In Hoshino Cave, we entered from a

191    natural entrance, which is not open to the public, and found an incomplete skeleton of one

192    individual of *Rhinolophus* sp. several meters below a paved commercial route (Fig. 1E).

193         Fragile bones were reinforced in the lab by coating with a solution of 5% Paraloid B-72

194    dissolved in acetone. They are stored at the National Museum of Nature and Science, Tokyo

195    (NMNS; Tsukuba, Ibaraki, Japan). A complete list of collected bones is provided in Table 1, and

196    a detailed taxonomic study of the specimens is in progress.

197         Some well-preserved fragments without secondary calcite crystal growth or acid etching

198    were consumptively sampled for radiocarbon dating; however, none preserved collagen (i.e., no

199    signal was detected for nitrogen using Elemental Analysis [EA] on a bone fragment), so these

200    materials were not useful for direct dating. Because we were unable to determine the age of any

201    individual fossil, we instead examined guano-like deposits accumulated in the same caves for

202    time-averaged $^{14}C$ ages.

203

204

205

206

207

208

209

**Guano-like deposits on Minami-Daito Island**

210

211      Guano-like deposits were sampled at four localities in Cave A (Fig. 1D) and one locality

212 in Hoshino Cave (Fig. 1E). These deposits are accumulated in piles on the floors of the caves

213 that can be washed downslope. They are soft muddy sediments brownish-black (10YR2/2 to

214 10YR2/3) to black (10YR2/1) in color. Mud particles are loosely coalesced to form sand-sized

215 granules, which are often contaminated with dolomite fragments. They are also present in local

216 small depressions above the floor. Flowstones in the caves are often colored black from pollution

217 in areas where the Japanese military used them as headquarters during World War II (WWII;

218 "Headquarter Hall" on the map) and where groundwater drains. We collected guano-like

219 deposits from large piles (Fig. 4A) or handpicked coalesced particles using forceps (Fig. 5A).

220 The largest pile of guano-like deposits (8~10m wide on the surface) was found in Hoshino Cave,

221 which is probably the deposit noted by Shimojana (1978). The thickness of the pile is over 50 cm

222 at a random spot where we collected samples from its bottom, a mid-part, and its top. There is no

223 sedimentological difference observed except that the bottom sample contained more carbonate

224 lithic fragments. In Cave A, a thin crust under a bat-lying flowstone was also sampled (Figs. 5B,

225 5D). The sampled deposits were dried in a convection oven at 38°C and were sieved at 850 μm,

226 425 μm, and 250 μm. Samples between 250 μm and 425 μm were carefully handpicked using

227 forceps for black particles to avoid carbonate contamination prior to further analyses.

228      Because insectivorous bats consume arthropods (crickets, beetles, moths, etc.), bat guano

229 contains their chitinous exoskeletons, which are resistant to decay. We utilized established

230 signals of the chitinous exoskeletons of arthropods to determine whether or not the guano-like

231 deposits are guano-derived by comparison with modern and fossil bat guanos as positive

232 references and red soil as a negative reference. The red soil was collected from the bottom of

233 thick soil deposits beneath a fissure in Cave A.

210   210

234

**Modern and subfossil bat guano as positive references**

235

236     For comparison with the guano-like deposits sampled in Hoshino Cave, we used a

237 commercial guano fertilizer collected in Indonesia (called R1 in figures; ARK Co. Ltd., Ushiku,

238 Ibaraki, Japan), modern bat guano of *Miniopterus fuliginosus* (R2) from an unnamed artificial

239 cave of soft sandstone in Taito, Isumi, Chiba, subfossil guano deposit (R3) from Fujido Cave in

240 Udeno, Gunma, and fecal pellets (R4) of *Vespertilio sinensis* in Chichibu, Saitama. Localities

241 were selected by Y.K. for ease of access. These samples were used as "positive references" for

242 comparison with our unknown guano-like samples from the Minami-Daito Island caves (see

243 Supplementary Article S1 for more details).

244

245

246 **Scanning Election Microscopy (SEM) observation**

247     In the fecal pellets of modern insectivorous bats, arthropod exoskeleton fragments are

248 usually observed. Thus, we imaged dry samples of the guano-like deposits from Hoshino Cave

249 and the four guano references at the National Museum of Nature and Science (NMNS; Tsukuba,

250 Ibaraki, Japan) using a JSM-6510 (JEOL Ltd., Tokyo, Japan) scanning electron microscope

251 (SEM) under 70x to 300x magnification. Images were taken at an acceleration voltage of 3 kV

252 with gold sputter coating on the dry samples.

253

254 **Fourier Transform Infrared Spectroscopy (FTIR)**

255     Fourier transform infrared (FTIR) spectroscopy is a technique commonly used to

256 characterize specific molecular structures in organic compounds. The FTIR spectra of chitin

257 extracted from modern and fossil guano as well as those of bulk guano are well known based on

258    previous studies (e.g., Wurster et al., 2010; Kaya et al., 2014), so we used FTIR to identify

259    whether chitin is a major component of the guano-like deposits. The hand-picked samples of the

260    guano-like deposits and reference materials (modern and fossil guano, red soil) were refluxed

261    with 1.0M HCl at 80°C for at least 8 hours to remove exogenous carbonates and organic acids

262    (e.g., fluvic acids) and were rinsed with deionized water until the solvent became a neutral pH.

263    After drying in a convection oven below 38°C, the samples were ground in an agate mortar with

264    a pestle. They were then stored in a desiccator at room temperature until analysis.

265         Each powdered sample was diluted with ground KBr, pressed into a pellet in a stainless-

266    steel disk, and analyzed without a vacuum using a JASCO FT/IR-6800 (JASCO Inc., Tokyo,

267    Japan) at NMNS. Pure KBr was measured as the background under the same conditions as the

268    samples. The infrared spectra of absorbance were measured from 400 cm$^{-1}$ to 4000 cm$^{-1}$ by 64

269    scans at a resolution of 4 cm$^{-1}$ and are expressed as the percentage of transmittance (%T).

270    Automatic baseline corrections were made using a second-degree polynomial fitting (x$^2$).

271

272    **Stable isotope analyses and C:N ratio of the guano-like samples**

273         To supplement FTIR results of the guano-like samples, we measured stable carbon and

274    nitrogen isotope values and mass ratios of organic carbon to nitrogen (C:N) for the HCl-treated

275    samples using a FLASH 2000 CHNS/O elemental analyzer coupled with a Finnegan MAT253

276    isotope ratio mass spectrometer (Thermo Fisher Scientific, Massachusetts, USA) at NMNS.

277    Isotopic ratios are expressed in delta notation ($\delta^{13}$C, $\delta^{15}$N) in parts per thousand (‰) and reported

278    on the VPDB scale for $\delta^{13}$C values and the AIR scale for $\delta^{15}$N values. For guano-like deposits, a

279    thick sample from Hoshino Cave and a handpicked pellet-like sample from Cave A were selected

280    for analysis. Three internal lab standards were analyzed for each run and used for data

281    correction. Repeated analyses of the standards were within ±0.2‰ for $\delta^{13}$C and ±0.25‰ for

282    $\delta^{15}N$. Carbon isotope values of guano references are used to reconstruct isotopic signals of their

283    diet by taking the following isotope fractionation factors into consideration. The fractionation

284    factor between the feces of insectivorous bats and their diet (i.e., insects) is known to be

285    negligible (Salvarina et al., 2013), whereas larger fractionation factors are observed between the

286    cuticles of insects and their diet of plant matter. In an experimental study, Gratton and Forbes

287    (2006) showed that tissues of predacious beetles are more enriched by 2.2‰ relative to their

288    aphid diet.

289

290    **Stable carbon isotopes of bone apatite**

291        Stable carbon isotope analysis of animal tissues is a useful technique to detect an isotopic

292    signal of $C_4$ plants in their habitat. Although no $C_4$ plant is native to the Daito Islands, historical

293    records (Editorial Committee of the History of Minami-Daito Village, 1990) document that the

294    $C_4$ perennial grass sugarcane was introduced on Minami-Daito Island in 1899–1900 and

295    increasingly replaced native $C_3$ forests on the island by the 1930s (see Introduction). We

296    therefore hypothesize that any organic materials on the island with the isotopic signature of $C_4$

297    plants must have originated after the introduction of sugarcane in 1899–1900. Thus, stable

298    carbon isotope analysis with correct applications of fractionation factors can serve as a time

299    constraint for direct human influences on Minami-Daito Island. Note that no scientific study such

300    as palynological analysis of sediment cores is available to independently validate the historical

301    documents.

302        Relatively well-preserved bat bones (no acid etching, no or limited calcite crystallization)

303    from Cave A were selected for carbon isotope analysis of bone apatite. For each bone, the

304    surface was shaved off to remove calcite crystals and carbonate deposits as much as possible

305    from the thin bones. The powdered samples were soaked in 2% NaOCl overnight for at least 12

306    hours at the room temperature. After rinsing with deionized water, they were treated with

307    buffered 0.1M acetic acid (pH=4.2) for 2 hours at 40°C until no obvious bubbles were observed,

308    and they were neutralized with ultrapure water and dried in an oven at 40 °C. The treated

309    samples were sent to Shoko Science Co., Ltd. (Saitama, Japan) and analyzed for stable carbon

310    isotope via a $H_3PO_4$ digestion using by a continuous flow Thermo Scientific Delta V Plus isotope

311    ratio mass spectrometer coupled to a Thermo Scientific GasBench II. Of the eight samples

312    analyzed in this study, seven come from individual bones, whereas one sample is composed of

313    multiple small bone fragments.

314        The carbon isotope values of bone apatite were used to reconstruct isotopic signals of

315    vegetation by applying experimentally known enrichment factors ($\varepsilon$*) and binary mixing

316    between $C_3$- and $C_4$-endmembers. The enrichment factor applied in this study is +11.0±0.1‰

317    between bone apatite and insectivorous diet (Podlesak et al., 2008). For isotopic spacing ($\Delta$)

318    between insectivorous diets of bats and surrounding vegetation, we applied +2.2‰ or +3.0‰

319    based on an a dietary-switch experimental study by Gratton and Forbes (2006). For the end-

320    members in binary mixing, $\delta^{13}C$ values of -12.5‰ and -29. 1‰ were used for pure $C_4$ (Cerling et

321    al., 1997) and $C_3$ vegetation, respectively. The latter was calculated based on the equation of

322    Kohn (2010), which takes mean annual precipitation (MAP), altitude, and latitude into account.

323    MAP of Minami-Daito Island between 1942 and 2020 was calculated as 1680 mm/year, which

324    was applied to the equation. See Supplementary Article S1 for more details.

325

326    **Radiocarbon dating of subfossil guano references**

327        We determined the $^{14}C$ age of both the fossil guano reference (R3) and the guano-like

328    samples for comparison. The same samples analyzed for stable isotopes were chosen for

329    radiocarbon dating. Prepared samples were sent to the accelerator mass spectrometry (AMS)

330    facility at the University Museum, the University of Tokyo, where the samples were further

331    prepared and measured by Compact AMS System (National Electrostatics Corp., Wisconsin,

332    USA), following their in-house protocols (Omori et al., 2017). For each sample, $\delta^{13}C$ measured

333    by AMS was used to correct for the conventional radiocarbon age (Stuiver and Polach, 1977).

334    These radiocarbon ages were calibrated by IntCal20 curves (Reimer et al., 2020) in OxCAL4.2

335    (Bronk Ramsey, 2009) and are expressed as calBP (Before Present; 0 calBP = AD 1950).

336    Preparation and analytical methods are described in Supplementary Article S1.

337

338

339

340

341

**RESULTS AND DISCUSSION**

343

**Skeletal remains of locally extinct cave-dwelling bats**

345    In a survey during the 1970s, Shimojana (1978) reported a few skeletons of *Rhinolophus*

346    sp. from Hoshino Cave. In this study, we found the skeletons of single individuals of

347    *Rhinolophus* sp. in both Hoshino Cave and Cave A. Additionally, we collected skeletons of

348    *Miniopterus* sp. from Cave A, which represent at least 13 individuals (taxonomic study in

349    progress). Some skeletons are articulated, but many are disconnected with associated bones

350    closely scattered on the surface of the cave floor (Fig. 2), so we infer that they were not

351    transported by water after death. No traces of soft tissues such as pelage are preserved. In Cave

352    A, we observed at least four individuals of *Miniopterus* sp. that were embedded within a thin

353    crust of flowstone (Fig. 3), two of which were collected. No fossil remains are permineralized,

354    but many are encrusted with calcite. The condition of calcite crystal growth on and in bones

355    depends on the availability of mineral-rich water flow near the bones. In many bone materials,

356    the surface is partially covered with small calcite crystals, and/or the medullary cavity of long

357    bones is partially infilled.

358    Due to the lack of bone collagen for radiocarbon dating in the specimens we sampled, it

359    is unknown whether these bat species utilized the cave contemporarily; however, because there is

360    no difference in bone preservation and secondary crystal growth of calcite between the two

361    species, our paleontological interpretation is that the ages of their existences do not differ even if

362    they may not be coeval *sensu stricto*.

363

364

**SEM observation of guano-like samples**

366    Fragments of insect exoskeletons are clearly visible in both modern (Figs. 4D-4E) and

367    fossil guano references (Fig. 4G) at or above 70x magnification although the fossil guano is

368    degraded to be humus-like and contaminated with sediments (Fig. 4F). On the other hand, the

369    guano-like samples appear to be aggregates of clay-sized particles with no clear presence of

370    insect remains (Figs. 4B-4C), suggesting that they may not be composed of bat guano.

371    Nevertheless, because the preservation potential of chitinous insect remains is expected to be

372    lower in guano deposits from tropical wet caves like those on Minami-Daito Island than in the

373    fossil guano reference collected from a more temperate region, we proceeded with further

374    analyses.

375

376

377    **FTIR**

378    None of the guano-like deposits collected in this study present spectral patterns

379    characteristic of fresh or fossil guano (Figs 6, 7, see Supplementary Article S1 for full

380    description of references). In the range between 1000 cm$^{-1}$ and 1800 cm$^{-1}$, different spectral

381    patterns are observed between guano references and sampled deposits. Particularly, a shoulder

382    peak at 1712 cm$^{-1}$ associated with C=O stretching of carboxylic acid (Dick et al., 2003) is present

383    in guano-like samples but does not occur in the spectra of guano references (Fig. 6). This peak

384    occurs in humified organic matter (Dick et al. 2003; Palumbo et al., 2018).

385    The FTIR spectrum of the guano-like sample Y180119g3 (Fig. 6D) is comparable to that

386    of humic acid (Figs. 6H-6I). The absorption at 1078 cm$^{-1}$ is ascribed to the stretching vibration of

387    oxygen bonds in aliphatic ether (Zhang et al., 2015). The presence of aliphatic compounds is

388    consistent with the interpretation that this sample is a fraction of humic substances (Méndez,

389    1967). The peak at 1244 cm$^{-1}$ can be interpreted as antisymmetric C-O stretching and OH

390 deformation in a carboxyl group, and -C-OH bending of phenols and tertiary alcohol in humic

391 substances (Dick et al., 2003). As organic functional groups, carboxylic acids are contained in

392 humic substances. We interpret that the guano-like deposits sampled in this study are forms of

393 humic substances rather than fossil bat guano, with the exception of Y160114g1, which was

394 identified as hydroxyapatite (Fig. 7D) by comparing characteristic spectral peaks with those of

395 pure hydroxyapatite in Jayaweera et al. (2018).

396      The hydroxyapatite sample, Y160114g1, occurs as a thin crust light brown in color only

397 partially exposed under a fracture of more recent flowstone on the slope of a large stalagmite

398 (Fig. 5B). Interestingly, we found skeletal remains of at least two individual bats lying on a slope

399 of the stalagmite, both of which are also covered by recent flowstone (Fig. 3B). The

400 hydroxyapatite crust stratigraphically underlies the bat skeleton. As a calcium phosphate mineral,

401 hydroxyapatite is commonly precipitated in caves where phosphorous-rich organic deposits such

402 as bat guano or bones are supplied and interaction between the guano-derived leachate and

403 calcium-rich water from carbonate host-rock can occur at a pH greater than 6 (Fiore and

404 Laviano, 1991; Hill and Forti 1997; Tămaş et al. 2014; Giurgiu and Tămaş, 2013). Because this

405 hydroxyapatite crust was found in association with a bat skeleton, and hydroxyapatite

406 precipitation is inhibited in the presence of humic and fluvic acids (Inskeep and Silvertooth,

407 1998), this crust was likely derived from bat guano rather than humified plant material.

408

409

410 **C:N ratios, $\delta^{13}$C, and $\delta^{15}$N values of the guano-like samples**

411      The C:N ratios, total nitrogen by weight percent (%N), $\delta^{13}$C values, and $\delta^{15}$N values of

412 the guano-like samples are shown in Fig. 8 (Tables 2, S1). In the bulk sample of the fissure-filled

413 deposit, total nitrogen is nearly 0.1%, which is within the standard range of nitrogen content for

414     sediments (Forbes and Bestland, 2006). The nitrogen content in the fecal pellet-like sample

415     Y180119g2 (Fig. 5A) from Cave A is lower than the %N range of guano references (Fig. 8A).

416     Because the FTIR spectrum of the pellet-like sample similarly traces that of the fissure-filled

417     deposit, we interpret that the fecal pellet-like sample is a mix of sediment and organic matter. In

418     general, C:N ratios of all analyzed samples are tightly clustered, ranging from 4.2 for fissure-

419     filled deposit to 6.5 for the fossil guano reference with the unknown guano-like samples (4.8 on

420     average) equivalent to those of modern guano (R1 and R2) (Fig. 8B). These values are much

421     lower than fresh plants and coals (e.g., Schmidt and Gleixner, 2005) and superficially meet one

422     of Forbes and Bestland's (2006) criteria to identify fossil guano (C:N <10). Nevertheless, in our

423     case, the low C:N values of the samples are still consistent with the FTIR-based classification of

424     the red soil of the Minami-Daito Islands as a lateritic soil because it is known that C:N ratios in

425     humic substances and soil organic matter extracted from modern lateritic soil show roughly

426     comparable values between 7 and 10 (Dick et al., 2003).

427         The $\delta^{13}C$ values of guano references range from -28.2‰ to -19.1‰, encasing the guano-

428     like samples (mean±1SD = -26.4±0.22‰) (Fig. 8B). Accounting for the isotopic spacing among

429     bat guano, their insectivorous diet, and surrounding vegetation, the guano-like deposits are well

430     within the range of $C_3$ plants, which exhibit a general range from -23‰ to -37‰ in non-desert

431     areas (Kohn, 2010). As they completely lack a signal of $C_4$ plants, we suggest that these deposits

432     were formed before anthropogenic influences because sugar cane, $C_4$ perennial grass, became

433     exclusively dominant by the 1930s due to heavy cultivation on the island.

434         The $\delta^{15}N$ values of the referenced guano samples widely range from 3.0‰ to 11.6‰,

435     placing the guano-like deposits from Hoshino Cave in its mid-range and the fecal pellet-like

436     sample from Cave A close to its upper limit (Fig. 8A). Forbes and Bestland (2006) used high

437   $\delta^{15}N$ values above 12‰ in association with low C:N ratios below 10 and high contents of

438   $SO_3+P_2O_5+CaO$ to identify a potential guano layer in accumulated cave deposits. The $\delta^{15}N$

439   values of the guano-like samples from Hoshino Cave do not meet their criteria although neither

440   do those of some guano references. Overall, as in the case of %N and C:N ratios, stable carbon

441   and nitrogen isotopes were not good indices to identify bat guano in caves of tropical islands

442   where lateritic soil can be developed.

443

444

445   **Stable carbon isotopes of bone apatite**

446

447   Bone apatite $\delta^{13}C$ values (n=8) show a wide range from -15.0‰ to -8.36‰ with a mean of -

448   11.5±2.38‰ (±1SD) (Table 3). Figure 9A shows estimated isotopic signals of vegetation,

449   calculated from carbon isotope values of bone apatite of bats. Considering that fractionation

450   factors and isotope values in the mixing model are reasonably assumed (see Supplementary

451   Article S1), $C_4$-feeding insects explains more than 10 % of the total diet in six out of the eight

452   individuals analyzed in this study even with a large isotopic spacing between predatory insects

453   and plants (open circle in Fig. 9A). On average, the estimated $\delta^{13}C$ value of bulk plants is -

454   25.4‰ (open circle), which is translated to 22% of $C_4$ plants in the simple mixing model. On

455   Minami-Daito Island, $C_4$ plants were introduced only by humans via sugarcane plantations.

456   Therefore, the unmistakable isotopic signal of $C_4$ plants demonstrates that these individuals

457   coexisted with humans after 1900.

458

459

460   **Group size and estimated ages of cave-dwelling bats on the Daito Islands**

461          Two locally extinct bat species, *Miniopterus* sp. and *Rhinolophus* sp., once existed in the

462    lifted atoll remotely located from the closest landmass. Based on the number of skeletal remains

463    recovered from Cave A in this study (at least n=17 for *Miniopterus* sp. and n=1 for *Rhinolophus*

464    sp.), this cave was utilized by more individuals of *Miniopterus* sp. than *Rhinolophus* sp.

465    Considering the taphonomic conditions of the Minami-Daito bats (unpermineralized, exposed on

466    cave floor without any depositional cover, fast crystal growth around bones in tropical wet

467    caves), we interpret that these skeletons are only a few thousand years old at most but probably

468    even younger and that the two species occurred contemporarily in the paleontological sense.

469          FTIR spectra and SEM images suggest that the guano-like deposits on Minami-Daito

470    Island are most reasonably humic substances, which are the final constituent of the

471    physicochemical degradation and microbial decomposition of organic matter, particularly plant

472    materials (Stevenson, 1994). The hydroxyapatite crust under the bat skeleton was possibly

473    formed from the interaction between bat guano and limestone/dolomite. Nevertheless, we reject

474    the null hypothesis that the "guano deposits" observed by Shimojana (1978) are fossil bat guano

475    and deny the presence of large amounts of guano deposits in the caves, which suggests the

476    skeletal remains are not resultant from large populations or those which utilized these caves for

477    generation after generation.

478          Our humic samples from both Hoshino Cave and Cave A yielded similar ages of 4565

479    calBP (on the 3-point average) and 4640 calBP, respectively (Table S2), which we think provide

480    the maximum age constraint for the bat species as the bat bones collected in this study were

481    scattered nearby pellet-like humic particles in Cave A. A better age constraint was provided by

482    stable carbon isotopes of the selected bat bones from Cave A. Isotopic signals of $C_4$ grass-

483    feeding insecs detected in various degrees from six out of eight individuals strongly indicate that

484    some of the sampled bats lived after 1900 (Fig. 9B).

485         In summary, small groups of bats that were dispersed to Minami-Daito Island did not

486    survive long due to strong anthropogenic stresses on the islands. Whether or not their arrivals

487    were caused by a single sporadic event or multiple events is still inconclusive in this study.

488    However, future taxonomic studies and analyses of morphological variation could elucidate the

489    possible biogeographic origins of the strayed populations, which would provide a hint to

490    understand how these species ended up co-occurring on the small island.

491

492

493    **Extirpation of two cave-dwelling bat species on the Daito Islands**

494         Our multiproxy approach to constrain the estimated ages of the Minami-Daito cave-

495    dwelling bats include hearing surveys of local residents on the Daito Islands. This survey was

496    conducted by Dr. Hidetoshi Ohta on August 22 and October 28 in 1991 for a different purpose

497    but happened to provide an imperfect yet interesting perspective regarding the extirpation of the

498    bats (pers. comm. with H. Ohta on December 31, 2018 by YK and DF). According to his field

499    notes, three men (Mr. Akamine, Mr. Nakama, Mr. Sunagawa; all in their 80s) commented that

500    they witnessed "bats smaller than the Daito flying fox" in a cave during the daytime within a few

501    years after the end of WWII. In the second survey, three other men (Mr. Toma, Mr. Suzuki, and

502    Mr. Okiyama; two in their 80s, one in his 90s) commented that they also saw "baby flying foxes"

503    in caves near "Hagu (rim)" before WWII. For local residents, the Daito flying fox is a typical

504    mammal on the island. Thus, these bats are reasonably considered as *Miniopterus* sp. and/or

505    *Rhinolophus* sp., as the Daito flying fox roosts in the canopies of trees during the daytime, not

506    utilizing caves. If our interpretation is correct, a remnant population of these bats persisted until

507   sometime after WWII, and the very last survivors could have been present until the 1950s, which

508   is consistent with our taphonomic interpretation of the bones.

509       On Minami-Daito Island, the irreversible rapid change from tropical/subtropical forests to

510   sugarcane fields was extraordinary following the arrival of early settlers/residents in 1899-1900

511   with heavy development by the 1930s. In addition to reducing favorable habitats for cave-

512   dwelling bats by opening the land and filling in sinkholes, there would have been other mortality

513   causes. Many caves were used as natural storage and air-raid shelters during WWII. Cave A was

514   a base of the Imperial Japanese Army during WWII. There are metal scraps, glass bottles, and

515   wood plausibly derived from that age. Surface water also transports waste into caves. We found

516   coal-like carbon particles in the guano-like samples while handpicking in the lab, which may be

517   related to wasted carbon derived from old steam locomotives that existed from 1917 to 1983 to

518   transport harvested sugarcane stalks as the railway track was run near Cave A (Kada, 2009).

519   Chemical pesticides were introduced in sugarcane plantations, and the aerial spray of pesticides

520   was conducted at least in the early 1970s (Editorial Committee of the History of Minami-Daito

521   Village, 1990: p.1167). Considering the extremely rapid development on the small island,

522   anthropogenic activities are undeniably responsible for the local extinctions of the last population

523   of the cave-dwelling bat species. It is noted however that the results of our study do not

524   completely exclude the possibility that these bats were non-viable drifting populations that

525   naturally died out without leaving descendants. In the future, this could be tested by finding out

526   how (and whether) other caves on the Daito Islands were utilized by the extirpated bats.

527

528   **Conservation paleobiology on tropical oceanic islands**

529     Using a multidisciplinary approach, we were able to bracket the estimated chronological

530   age of the Minami-Daito cave-dwelling bats, ranging from a maximum constrained age of 4,640

531   calBP (radiocarbon age of humin closely scattered with the bat bones in Cave A) to the 1950s

532   (hearing survey). Stable carbon isotopes of bone apatite provided unmistakable direct evidence

533   that they existed after 1900 and reinforced the hearing survey record.

534     Despite rapid civilization and deforestation on the island throughout the 20th century, the

535   Daito flying fox has been able to survive on the island. The Daito flying fox, which is designated

536   as a critically endangered subspecies (IA) in the National Red Data List of the Ministry of the

537   Environment, Japan (RDB, 2020) and is thus of high concern for species conservation (Vincenot

538   et al., 2017), consumes fruits and nectar of native species such as Chinese banyan (*Ficus*

539   *microcarpa*), *Fiscus superba* var. *japonica*, *Ficus virgala*, and fan palm trees (*Livistoma*

540   *chinensis* var. *amanoi*), but it also utilizes windbreak trees and street trees as a food source

541   (Kinjo, 2009). Flexible food preferences may explain how the Daito flying fox has survived

542   throughout anthropogenic damages as in the case of the neighboring subspecies Orii's flying fox

543   (*Pteropus dasymallus inopinatus*) on Okinawa Island, which utilizes planted trees in urban areas

544   as stable food sources (Nakamoto et al., 2007).

545     Regarding the presence of fossil bat species on an oceanic island, a similar case was

546   reported for an extinct endemic bat, *Synemporion keana* (lava-tube bat), from the Hawaiian

547   Islands, which are over 3800 km away from the nearest continental landmass (Ziegler et al.,

548   2016). *Synemporion keana* is a vespertilionid bat slightly smaller than the extant Hawaiian hoary

549   bat (*Lasiurus cinereus semotus*) that is known to have inhabited the Hawaiian Islands at least

550   until the earliest Polynesian cultural period because a fossil of *S. keana* was successfully

551   radiocarbon dated to 1670 BP (Ziegler et al., 2016). According to that study and the references

552 therein, those fossils were recovered from infilled deposits (soil, eolian deposit, pond deposit) or

553 exposed on the floor of limestone sinkholes, volcanic lava tubes, a piping cave, and a volcanic-

554 tuff cone crater. Similar to our studies, those fossils were not suitable for DNA extraction or

555 radiocarbon dating. They estimated a chronological range of the Hawaiian fossil bat species by

556 establishing the $^{14}$C ages of both coexisting animal skeletons such as birds and rats and cultural

557 artifacts derived from the same stratigraphic level or nearby and the formation of volcanic caves

558 from which the fossils were found. Another interesting case of the late Holocene (<4,000 BP)

559 extirpation of bats is found on a tropical island in the Caribbean (Soto-Centeno and Steadman,

560 2015).

561 In this study, we revealed that two cave-dwelling bat species were extirpated from

562 Minami-Daito Island without any zoological record when they existed. Minami-Daito Island

563 used to be a home of three bat species, but only a single species survived anthropogenic

564 disturbance. Geological, geochemical, and paleontological approaches are useful to bracket

565 chronological ranges of the two extirpated species. Chronological ranges of extirpated species

566 should be estimated with higher accuracy to deduce causality of the local extinction events and

567 subsequently to promote conservation of biodiversity on oceanic islands, which are generally

568 vulnerable to anthropogenic factors.

569

570

571 **Conclusions**

572 Minami-Daito Island is an oceanic island that has never been connected to another

573 landmass since its emergence. A few skeletons of *Rhinolophus* sp. were found during the 1970s

574 from Hoshino Cave, the only tourist cave on the island (Shimojana, 1978). In this study, we

575 found not only an additional skeleton of *Rhinolophus* sp. from Hoshino Cave but also a skeleton

576  of the same species and more of *Miniopterus* sp. from another private cave. Because these bones,

577  which were exposed on the floor of the tropical dolomite caves, did not preserve collagen for

578  radiocarbon dating, we used multidisciplinary proxies to provide time constraints for estimated

579  ages of the bats. Differing from a previous study, we obtained limited witnesses of cave-dwelling

580  bats from before/during WWII and concluded the "guano-like" deposits commonly previously

581  identified were humic substances formed ca. 4640 calBP, which gives the maximum age

582  constraint for the extirpated bats. Their populations were never large and quickly shrank due to

583  rapid and heavy deforestation for sugarcane plantations on the island. They were extirpated from

584  Minami-Daito Island without any zoological record when they existed. This study highlights that

585  anthropogenic activities increase the mortality of animal species newly strayed into insular

586  environments.

587

588

589  **Acknowledgments**

590      We deeply appreciate Shin-Ichiro Kawada (National Museum of Nature and Science,

591  Japan for permitting us to access zoological collections at NMNS and assisting with fieldwork

592  and Benjamin T. Breeden III (University of Utah) for providing constructive comments and

593  English proofreading for the early draft. We are thankful to Katsuji Yoshida (Cave Exploration

594  Pro-Guide Team Ciao!), Takeshi Matsushita (Cave Exploration Pro-Guide Team Ciao!), and

595  Yukari Yamaguchi (Cave Exploration Pro-Guide Team Ciao!) for making a route map of Cave A

596  and to Ken Ōyabu and Masaharu Hayakawa (Uekusa Gakuen University & Junior College) for

597  permitting access to modern bat guano in Taito, Isumi, Chiba. We are grateful to Yushi Osawa,

598  Keiko Osawa, Yu Iijima, and Hiroko Nagaoka for field assistance and to Mika Yagishita and

599  Sonoko Suzuki for lab assistance. Nozomi Suzuki provided us great support for isotope analyses.

600   We thank Brandon Hedrick for carefully handling our manuscript and J. Angel Soto-Centeno and

601   one anonymous reviewer for constructive comments on the early draft, which improved the

602   quality of the manuscript.

603

604

605   This project was conducted as part of project I+D+i PID2020-117289GBI00 funded by MCIN/

606   AEI/10.13039/501100011033/. Y.K. was financially supported by the Fujiwara Natural History

607   Foundation (2018), the National Museum of Nature and Science as part of a research project

608   called "Chemical Stratigraphy and Dating as a Clue for Understanding the History of the Earth

609   and Life", JSPS KAKENHI Grant Number 18K13650, and the Generalitat de Catalunya

610   (CERCA Programme). D.F. was financially supported by the 26th PRO NATURA FUND, Asahi

611   Glass Foundation, and JSPS KAKENHI Grant Number 20H01979.

612    **Figure Captions**

613

614    **Figure 1**. Map of Minami-Daito Island, route map of a privately-owned Cave A, cave map of

615    Hoshino Cave. (A) Satellite map (Google Earth, 2020); (B) Map of Ryukyu Islands; (C)

616    Entrance of Cave A; (D) Route map of Cave A; (E) Map of Hoshino Cave (Simplified from a

617    map of Ehime University Expedition Club, 1972). Solid circles indicate sampling localities of

618    guano-like deposits, and open stars indicate sampling localities of cave-dwelling bat bones.

619    **Figure 2.** Various conditions of skeletal remains of *Miniopterus* sp. (A) partially articulated, not

620    covered by flowstone; (B) complete skull with fragmentary bones, not covered by flowstone; (C)

621    partially articulated, covered by flowstone on the cave floor; (D) almost fully articulated,

622    covered by flowstone (NMNS-PV 23770).

623    **Figure 3.** Skeletal remains of *Miniopterus* sp. on the slopes of stalagmite in Cave A. (A) Heavily

624    covered by stalagmite; (B) More heavily covered by stalagmite, whose locality is shown in Fig.

625    1D.

626    **Figure 4**. Optic and SEM images of guano references and guano-like deposit in Hoshino Cave.

627    (A-C) Guano-like deposit (H180120g5) collected from Hoshino Cave, Minami-Daito Island; (D,

628    E) Modern guano (R2) collected in Taito, Chiba; (F, G) Fossil guano (R3) collected in Fujido

629    Cave, Gunma.

630    **Figure 5**. SEM and optical images of guano-like deposit in Cave A. (A, C) Fecal pellet-like

631    sample (Y180119g2). (B, D) Hydroxyapatite crust (Y160114g1), possibly derived from bat

632    feces.

633    **Figure 6**. FTIR spectra of guano references, guano-like deposits, and humic acid. (A)

634    Commercial fertilizer (R1); (B) Modern fecal pellet (R3); (C) Fossil guano (R4); (D, E) Guano-

635    like deposits sampled in Cave A; (F, G) Guano-like deposits sampled in Hoshino Cave; (H)

636    humic acid (Dick et al., 2003); (I) humic acid extracted from municipal solid waste (Palumbo et

637    al., 2018). The numbers of Minami-Daito samples (4: Y180119g3, 5: Y180120g1, 6:

638    H180120g5) correspond to sampling localities in Figs. 1D-1E. u: upper, b: bottom.

639  **Figure 7.** FTIR spectra of lateric soil, fissure-filled deposit, sampled deposits, and

640  hydroxyapatite. (A) Whole soil of Latosol (Dick et al., 2003); (B) Fissure-filled deposit; (C)

641  Guano-like deposit; (D) Hydroxyapatite crust; (E) Hydroxyapatite (Jayaweera et al., 2008). The

642  numbers of Minami-Daito samples (1: Fissure-filled deposit, 2: Y160114g1, 3: Y180119g2)

643  correspond to sampling localities in Fig. 1D.

644  **Figure 8**. Isotopic composition of carbon and nitrogen, total nitrogen by weight percent (%N),

645  and C:N ratio in the selected guano-like samples and guano references, corresponding to Table 2.

646  (A) Stable nitrogen isotope values vs. %N; (B) Stable carbon isotope values vs. C:N. u: upper,

647  m: middle, b: bottom. Raw data are provided in Table S1. A full description of the bat guano

648  references (R1-R4) is in Supplementary Article S1.

649  **Figure 9**. Estimated $\delta^{13}$C values of vegetation based on bone apatite of cave-dwelling bats and

650  chronological ranges of the extirpated bats on Minami-Daito Island. (A) Estimated $\delta^{13}$C values

651  of vegetation on Minami-Daito Island, calculated from bone apatite $\delta^{13}$C values of the cave-

652  dwelling bats. Measured $\delta^{13}$C values of bone apatite are provided in Table 3. For the isotopic

653  enrichment factors and $\delta^{13}$C values of pure $C_3$- and $C_4$-vegetation applied in this study, see

654  Supplementary Article S1 for details. (B) Estimated ages of the extirpated Minami-Daito bats

655  with lines of evidence revealed by this study. Thicker and darker lines indicate the time range

656  that is more strongly supported.

657

658  **Table Captions**

659

660  **Table 1.** A list of skeletal remains of *Miniopterus* sp. and *Rhinolophus* sp. collected from

661  Minami-Daito Island, Okinawa. At the National Museum of Nature and Science (Tokyo, Japan),

662  all vertebrate fossils cataloged in the Department of Geology and Paleontology start with the

663  prefix "NMNS-PV".

664

665   **Table 2.** Summary of carbon and nitrogen isotopes, C:N ratios, weight percent of carbon and

666   nitrogen in guano-like samples.

667

668   **Table 3.** Stable carbon isotope values of bone apatite in the Minami-Daito cave-dwelling bats.

669

670   **Supplementary Information**

671   **Table S1**. Isotopic composition of carbon and nitrogen, total nitrogen by weight percent (%N),

672   and C:N ratio in selected guano-like samples and guano references, corresponding to Table 2 and

673   Fig. 8.

674   **Table S2**. Summary of radiocarbon ages (calBP) of a fossil guano reference and Minami-Daito

675   samples.

676

677

678

679

680

681

682   **References**

683

684   Albert JS, Schoolmaster DR, Tagliacollo V, Duke-Sylvester SM. 2017. Barrier displacement on

685       a neutral landscape: Toward a theory of continental biogeography. *Systematic Biology*

686       66(2): 167–182. DOI 10.1093/sysbio/syw080.

687

688    Allentoft ME, Heller R, Oskam CL, Lorenzen ED, Hale ML, Gilbert MTP, Jacomb C, Holdaway

689        RN, Bunce M. 2014. Extinct New Zealand megafauna were not in decline before human

690        colonization. *Proceedings of the National Academy of Sciences of the United States of*

691        *America* 111(13):4922–4927. DOI 10.1073/pnas.1314972111.

692

693

694    Bronk Ramsey C. 2009. Bayesian analysis of radiocarbon dates. *Radiocarbon* 51(1): 337–360.

695        DOI 10.1017/S0033822200033865.

696    Carpenter JK, Wilmshurst JM, McConkey KR, Hume JP, Wotton DM, Shiels AB, Burge OR,

697        Drake DR. 2020. The forgotten fauna: Native vertebrate seed predators on islands.

698        *Functional Ecology* 34(9): 1802–1813. DOI 10.1111/1365-2435.13629.

699

700    Cerling TE, Harris JM, MacFadden BJ, Leakey MG, Quade J, Eisenmann V, Ehleringer JR.
701        1997. Global vegetation change through the Miocene/Pliocene boundary. *Nature* 389: 153–
702        158. DOI 10.1038/38229.

703

704    Chen SF, Juan C, Rossite S, Kinjo T, Fukui D, Kawai K, Tsang SM, Veluz MJ, Sakurai H, Jang-

705        Liaw NH, Osawa K, Ko WY, Izawa M. 2021. Population genetic structure of the insular

706        Ryukyu flying fox *Pteropus dasymallus*. *Biotropica* 3: 979211. DOI 10.1111/btp.12897.

707    Dick DP, Santos JHZ, Ferranti EM. 2003. Chemical Characterization and Infrared Spectroscopy

708        of Soil Organic Matter from Two Southern Brazilian Soils. *Revista Brasileira de Ciência do*

709        *Solo* 27(1): 29–39. DOI 10.1590/s0100-06832003000100004.

710    Editorial Committee of the History of Minami-daito Village. 1990. [The History of Minami-daito

711        Village]. A revised edition. Minami-daito Village Office, Naha [in Japanese]

712    Ehime University Expedition Club. 1972. [Caves on Minami-Daito Island]. Report on the 8th

713        Exploration of the Ryukyu Islands. [in Japanese]

714    Fiore S, Laviano R. 1991. Brushite, hydroxylapatite, and taranakite from Apulian caves

715        (southern Italy): New mineralogical data. *American Mineralogist* 76(9–10): 1722–1727.

716    Forbes MS., Bestland, EA. 2006. Guano-derived deposits within the sandy cave fills of

717        Naracoorte, South Australia. *Alcheringa: An Australasian Journal of Palaeontology* 1: 129–

718        146. DOI 10.1080/03115510609506859.

719    Giurgiu A, Tămaş, T. 2013. Mineralogical data on bat guano deposits from three Romanian

720        caves. *Studia Universitatis Babes-Bolyai, Geologia* 58(2): 13–18. DOI 10.5038/1937-

721        8602.58.2.2.

722    Google Earth V7.3.3.7786 (July 21, 2020) Minami-Daito, Okinawa, Japan. 25 50'27.86"N, 131

723    14'35.24"E, Eye alt 11.81km. Landsat/Copernicus, Maxar Technologies 2021, CNES/Airbus

724    2012. http://www.earth.google.com [accessed May 17, 2021].

725   Gratton C, Forbes AE. 2006. Changes in $\delta^{13}$C stable isotopes in multiple tissues of insect

726        predators fed isotopically distinct prey. *Oecologia* 147(4): 615–624. DOI 10.1007/s00442-

727        005-0322-y.

728   Hill CA, Forti P. 1997. Cave Minerals of the World, second edition. Huntsville, Alabama:

729        National Speleological Society, 463 p.

730   Inskeep WP, Silvertooth JC. 1998. Inhibition of hydroxyapatite precipitation in the presence of

731        fulvic, humic, and tannic acids. *Soil Science Society of America Journal* 52: 941–946.

732   Jayaweera HDAC, Siriwardane I, de Silva KMN, de Silva RM. 2018. Synthesis of

733        multifunctional activated carbon nanocomposite comprising biocompatible flake nano

734        hydroxyapatite and natural turmeric extract for the removal of bacteria and lead ions from

735        aqueous solution. *Chemistry Central Journal* 12(1): 1–14. DOI 10.1186/s13065-018-0384-

736        7.

737   Kada Y. 2009. Remember sugarcane railway on Minami-Daito Island. In: [The People and

738        Nature of Minami Daito Island]. Ed. Seiichi Nakai, Kazuaki Higashi and Daniel Long,

739        104–120. Kagoshima: Nampo Shinsha. [in Japanese]

740   Kaya M, Seyyar O, Baran T, Turkes T. 2014. Bat guano as new and attractive chitin and chitosan

741        source. *Frontiers in Zoology* 11: 59. DOI 10.1186/s12983-014-0059-8.

742   Kinjo K. 2009. [Bats Living in a Remote Oceanic Island]. In: [The People and Nature of Minami

743        Daito Island]. Ed. Seiichi Nakai, Kazuaki Higashi and Daniel Long, 138–150. Kagoshima:

744        Nampo Shinsha. [in Japanese]

745  Klein GV, Kobayashi K. 1980. Geological summary of the North Philippine Sea, based on Deep

746      Sea Drilling Project Leg 58 Results. In Klein GV, Kobayashi K., eds. *Initial Reports of the*

747      *Deep Sea Drilling Project 58*. U.S. Government Printing Office, 951–961. DOI

748      10.2973/dsdp.proc.58.144.1980.

749  Kohn MJ 2010. Carbon isotope compositions of terrestrial C3 plants as indicators of

750      (paleo)ecology and (paleo)climate. *Proceedings of the National Academy of Sciences of the*

751      *United States of America* 107(46): 19691–19695. DOI 10.1073/pnas.1004933107.

752  Méndez J. 1967. Organic compounds in humic acid extracts. *Geoderma* 1(1): 27–36. DOI

753      10.1016/0016-7061(67)90012-2.

754  Nakamoto A, Kinjo K, Izawa M. 2007. Food habits of Orii's flying-fox, *Pteropus dasymallus*

755      *inopinatus*, in relation to food availability in an urban area of Okinawa-jima Island, the

756      Ryukyu Archipelago, Japan. *Acta Chiropterologica* 9(1): 237–249. DOI 10.3161/1733-

757      5329(2007)9[237:FHOOFP]2.0.CO;2.

758  Nambu A, Inagaki S, Ozawa S, Suzuki Y, Iryu Y. 2003. Stratigraphy of reef deposits on Kita-

759      daito-jima, Japan. *Journal of Geological Society of Japan* 109(11): 617–634. [in Japanese

760      with English summary]

761  Ohde S., Elderfield H. 1992. Strontium isotope stratigraphy of Kita-daito-jima Atoll, North

762      Philippine Sea: implications for Neogene sea-level change and tectonic history. *Earth and*

763      *Planetary Science Letters* 113(4): 473–486. DOI 10.1016/0012-821X(92)90125-F.

764    Omori T, Yamazaki K, Itahashi Y, Ozaki H, Yoneda M. 2017. Development of a simple

765      automated graphitization system for radiocarbon dating at the University of Tokyo. 14th

766      International Conference on Accelerator Mass Spectrometry, University of Ottawa,

767      Canada.

768    Ota Y, Omura A, Koba M, Kawana T, Miyauchi T. 1991. Late Quaternary tectonic movements

769      as deduced from raised coral reefs of Daito Islands on the northwestern part of Philippine

770      Sea Plate. *Journal of Geography* 100(3): 317–336. [in Japanese with English summary]

771    Palumbo G, Schiavon M, Nardi S, Ertani A, Celano G, Colombo CM. 2018. Biostimulant

772      potential of humic acids extracted from an amendment obtained via combination of olive

773      mill wastewaters (OMW) and a pre-treated organic material derived from municipal solid

774      waste (MSW). *Frontiers in Plant Science* 9: 1028. DOI 10.3389/fpls.2018.01028.

775    Podlesak DW, Torregrossa A-M, Ehleringer JR, Dearing MD, Passey BH, Cerling TE. 2008.

776      Turnover of oxygen and hydrogen isotopes in the body water, $CO_2$, hair, and enamel of a

777      small mammal. *Geochimica et Cosmochimica Acta* 72: 19–35. DOI

778      10.1016/j.gca.2007.10.003.

779    RDB, 2020. [Japanese Red Data Book]. Japan Integrated Biodiversity Information System.

780    Reimer P, Austin WEN, Bard E, Bayliss A, Blackwell PG, Bronk Ramsey C, Butzin M, Cheng

781      H, Lawrence Edwards R, Friedrich M, Grootes PM, Guilderson TP, Hajdas I, Heaton TJ,

782      Hogg AG, Hughen KA, Kromer B, Manning SW, Muscheler R, ... Talamo, S. (2020). The

783      IntCal20 Northern Hemisphere radiocarbon age calibration curve (0-55 cal kBP).

784      *Radiocarbon* 62(4): 725-757. DOI 10.1017/RDC.2020.41.

785 Salvarina I, Yohannes E, Siemers BM, Koselj K. 2013. Advantages of using fecal samples for

786     stable isotope analysis in bats: Evidence from a triple isotopic experiment. *Rapid*

787     *Communications in Mass Spectrometry* 27(17): 1945–1953. DOI 10.1002/rcm.6649.

788 Schmidt MWI, Gleixner G. 2005. Carbon and nitrogen isotope composition of bulk soils,

789     particle-size fractions and organic material after treatment with hydrofluoric acid. *European*

790     *Journal of Soil Science* 56(3): 407–416. DOI 10.1111/j.1365-2389.2004.00673.x.

791 Seno T, Maruyama S. 1984. Paleogeographic reconstruction and origin of the Philippine Sea.

792     *Tectonophysics* 102: 53–84. DOI 10.1016/0040-1951(84)90008-8.

793 Shimojana M. 1978. [Cave faunas on Minami- and Kita-daito-jima Islands and the southern part

794     of Okinawa-jima Island]. In: Board of Education, Okinawa Prefecture, ed. [Survey Report

795     on Caves in Okinawa Prefecture I]. Board of Education, Okinawa Prefecture, Naha, 75-

796     111. [in Japanese]

797 Soto-Centeno JA, Steadman, DW. 2015. Fossils reject climate change as the cause of extinction

798     of Caribbean bats. *Scientific Reports* 5: 7971. DOI 10.1038/srep07971.

799 Stevenson FJ. 1994. Humus Chemistry: Genesis, Composition, Reactions (2nd ed.). New York:

800     John Wiley & Sons.

801 Stuiver M, Polach HA. 1977. Discussion reporting of $^{14}$C data. *Radiocarbon* 19(3): 355–363.

802 Tămaş T, Miheţ O, Giurgiu A. 2014. Mineralogy of bat guano deposits from Huda lui papară

803     cave (Trascău Mountains, Romania). *Carpathian Journal of Earth and Environmental*

804     *Sciences* 9(3): 25–32.

805  Urushibara-Yoshino K. 2012. Karstification processes on Minamidaito Island in the Nansei

806       Archipelago, southwest Japan. *Bulletin of the Faculty of Letters, Hosei University* 65: 83–

807       95. [in Japanese with English summary]

808  van der Geer A, Lyras G, de Vos J, Dermitzakis D. 2010. *Evolution of Island Mammals:*

809       *Adaptation and Extinction of Placental Mammals on Islands*. Oxford: Wiley-Blackwell.

810       DOI 10.1002/9781444323986.

811  Vincenot CE, Collazo AM, Russo D. 2017. The Ryukyu flying fox (*Pteropus dasymallus*)—A

812       review of conservation threats and call for reassessment. *Mammalian Biology* 83: 71–77.

813       DOI 10.1016/j.mambio.2016.11.006.

814  Wood JR, Alcover JA, Blackburn TM, Bover P, Duncan RP, Hume JP, Louys J, Meijer HJM,

815       Rando JC, Wilmshurst JM. 2017. Island extinctions: Processes, patterns, and potential for

816       ecosystem restoration. *Environmental Conservation* 44(4):348–358. DOI

817       10.1017/S037689291700039X.

818

819  Wurster CM, Bird MI, Bull ID, Creed F, Bryant C, Dungait JAJ, Paz V. 2010. Forest contraction

820       in north equatorial Southeast Asia during the Last Glacial Period. *Proceedings of the*

821       *National Academy of Sciences* 107(35): 15508–15511. DOI 10.1073/pnas.1005507107.

822  Zhang W, Jiang S, Wang K, Wang L, Xu Y, Wu Z, Shao H, Wang Y, Miao M. 2015.

823       Thermogravimetric dynamics and FTIR analysis on oxidation properties of low-rank coal at

824  low and moderate temperatures. *International Journal of Coal Preparation and Utilization*

825  35(1): 39–50. DOI 10.1080/19392699.2013.873421.

826 Ziegler AC, Howarth FG, Simmons NB. 2016. A second endemic land mammal for the

827  Hawaiian Islands: a new genus and species of fossil bat (Chiroptera: Vespertilionidae).

828  *American Museum Novitates* 3854: 1–52.

829

830

831

832

833

834

835

# Figure 1

Figure 1. Map of Minami-Daito Island, route map of a privately-owned Cave A, cave map of Hoshino Cave.

(A) Satellite map (Google Earth, 2020); (B) Map of Ryukyu Islands; (C) Entrance of Cave A; (D) Route map of Cave A; (E) Map of Hoshino Cave (Simplified from a map of Ehime University Expedition Club, 1972). Solid circles indicate sampling localities of guano-like deposits, and open stars indicate sampling localities of cave-dwelling bat bones.

A

Hoshino Cave

Cave A

B

Okinawa Island

Kita-Daito Island

Minami-Daito Island

200 km

C

D

bat-lying
stalagmite
(Fig. 3B)

continued

underground lake

To ground

"Headquater Hall"

N

depression

To ground?

Sampling locality
1: Fissure-filled deposit (soil)
2: Y160114g1
3: Y180119g2     Guano-like
4: Y180119g3     deposit
5: Y180120g1
☆ Sampling locality of bat bones
— Route track
◖ Boulder breccia

To ground?

To ground?

privately-owned Cave A
natural entrance

To
ground?

0          10m

E

N

Sampling locality
Guano-like deposit
● 6: H180120g5
☆ Sampling locality of bones

☆

paved route

Commercial tour
entrance

Hoshino Cave
entrance

0   10  20  30  40  50m

# Figure 2

Figure 2. Various conditions of skeletal remains of *Miniopterus* sp.

(A) partially articulated, not covered by flowstone; (B) complete skull with fragmentary bones, not covered by flowstone; (C) partially articulated, covered by flowstone on the cave floor; (D) almost fully articulated, covered by flowstone (NMNS-PV 23770).
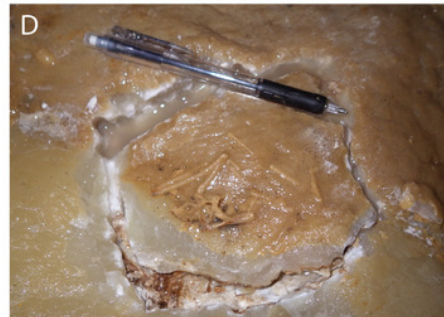
# Figure 3

Figure 3. Skeletal remains of *Miniopterus* sp. on the slopes of stalagmite in Cave A.

(A) Heavily covered by stalagmite; (B) More heavily covered by stalagmite, whose locality is shown in Fig. 1D.
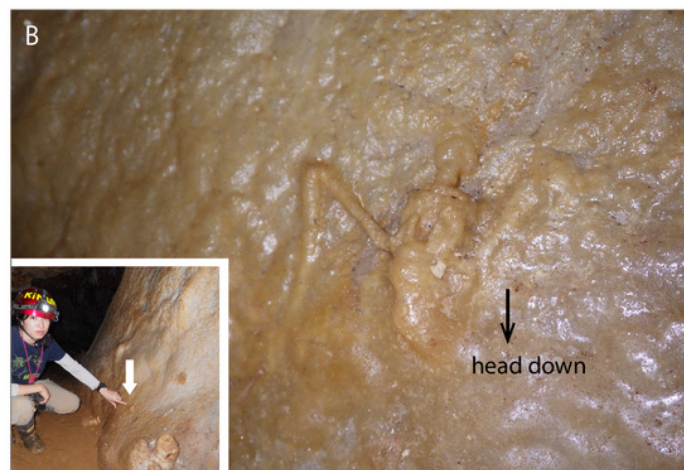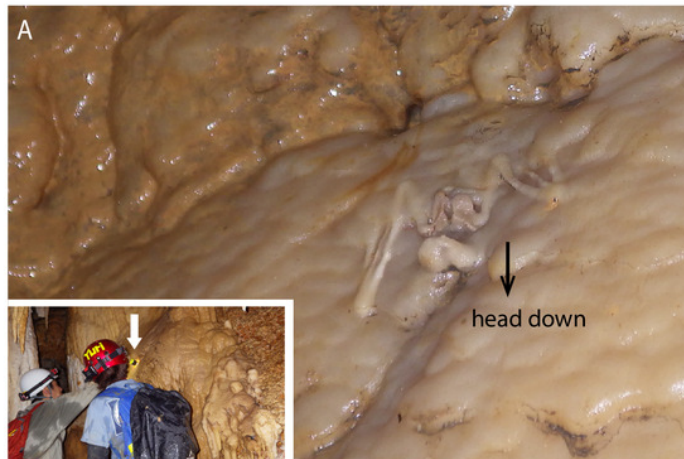
# Figure 4

Figure 4. Optic and SEM images of guano references and guano-like deposit in Hoshino Cave.

(A-C) Guano-like deposit (H180120g5) collected from Hoshino Cave, Minami-Daito Island; (D, E) Modern guano (R2) collected in Taito, Chiba; (F, G) Fossil guano (R3) collected in Fujido Cave, Gunma.
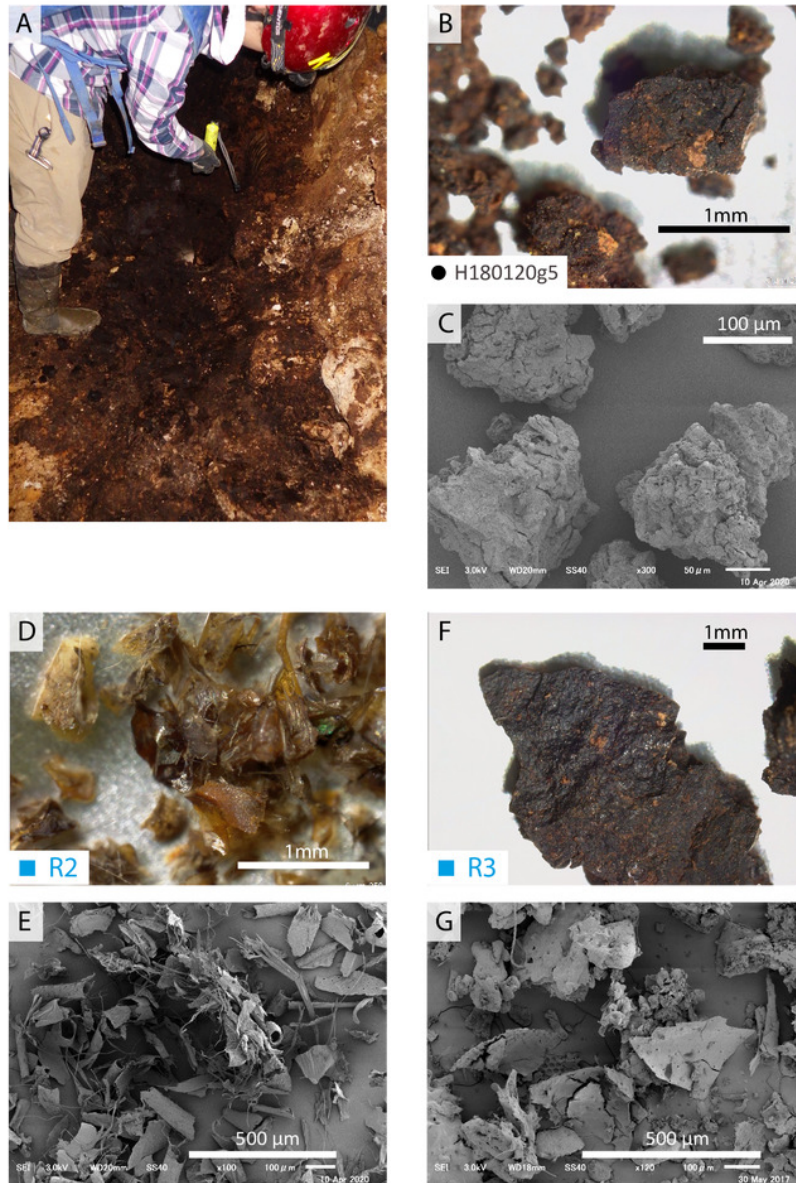
# Figure 5

Figure 5. SEM and optical images of guano-like deposit in Cave A.

(A, C) Fecal pellet-like sample (Y180119g2). (B, D) Hydroxyapatite crust (Y160114g1), possibly derived from bat feces.
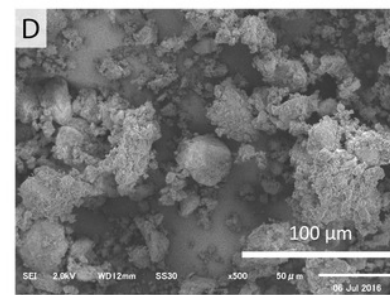
# Figure 6

Figure 6. FTIR spectra of guano references, guano-like deposits, and humic acid.

(A) Commercial fertilizer (R1); (B) Modern fecal pellet (R3); (C) Fossil guano (R4); (D, E) Guano-like deposits sampled in Cave A; (F, G) Guano-like deposits sampled in Hoshino Cave; (H) humic acid (Dick et al., 2003); (I) humic acid extracted from municipal solid waste (Palumbo et al., 2018). The numbers of Minami-Daito samples (4: Y180119g3, 5: Y180120g1, 6: H180120g5) correspond to sampling localities in Figs. 1D-1E. u: upper, b: bottom.
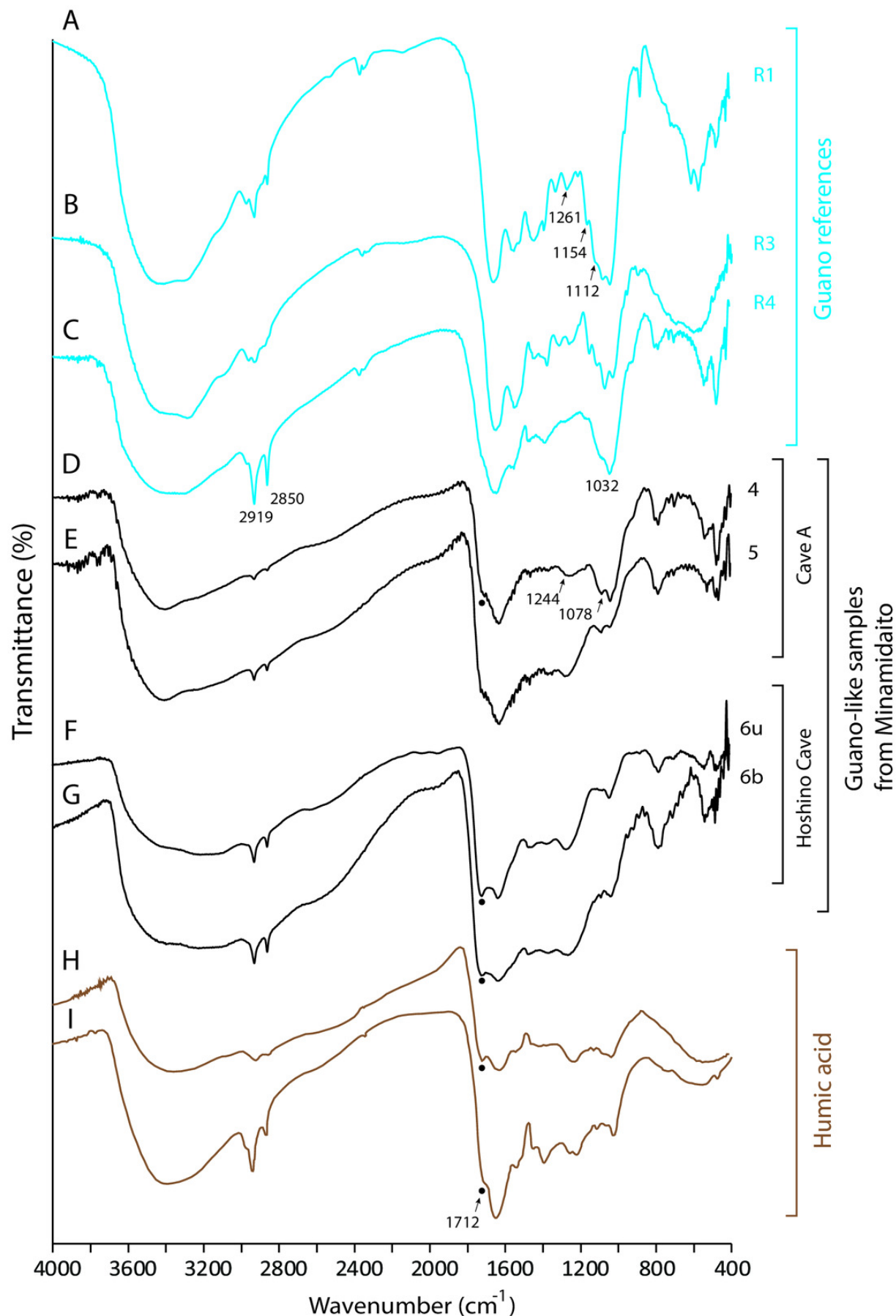
# Figure 7

Figure 7. FTIR spectra of lateric soil, fissure-filled deposit, sampled deposits, and hydroxyapatite.

(A) Whole soil of Latosol (Dick et al., 2003); (B) Fissure-filled deposit; (C) Guano-like deposit; (D) Hydroxyapatite crust; (E) Hydroxyapatite (Jayaweera et al., 2008). The numbers of Minami-Daito samples (1: Fissure-filled deposit, 2: Y160114g1, 3: Y180119g2) correspond to sampling localities in Fig. 1D.
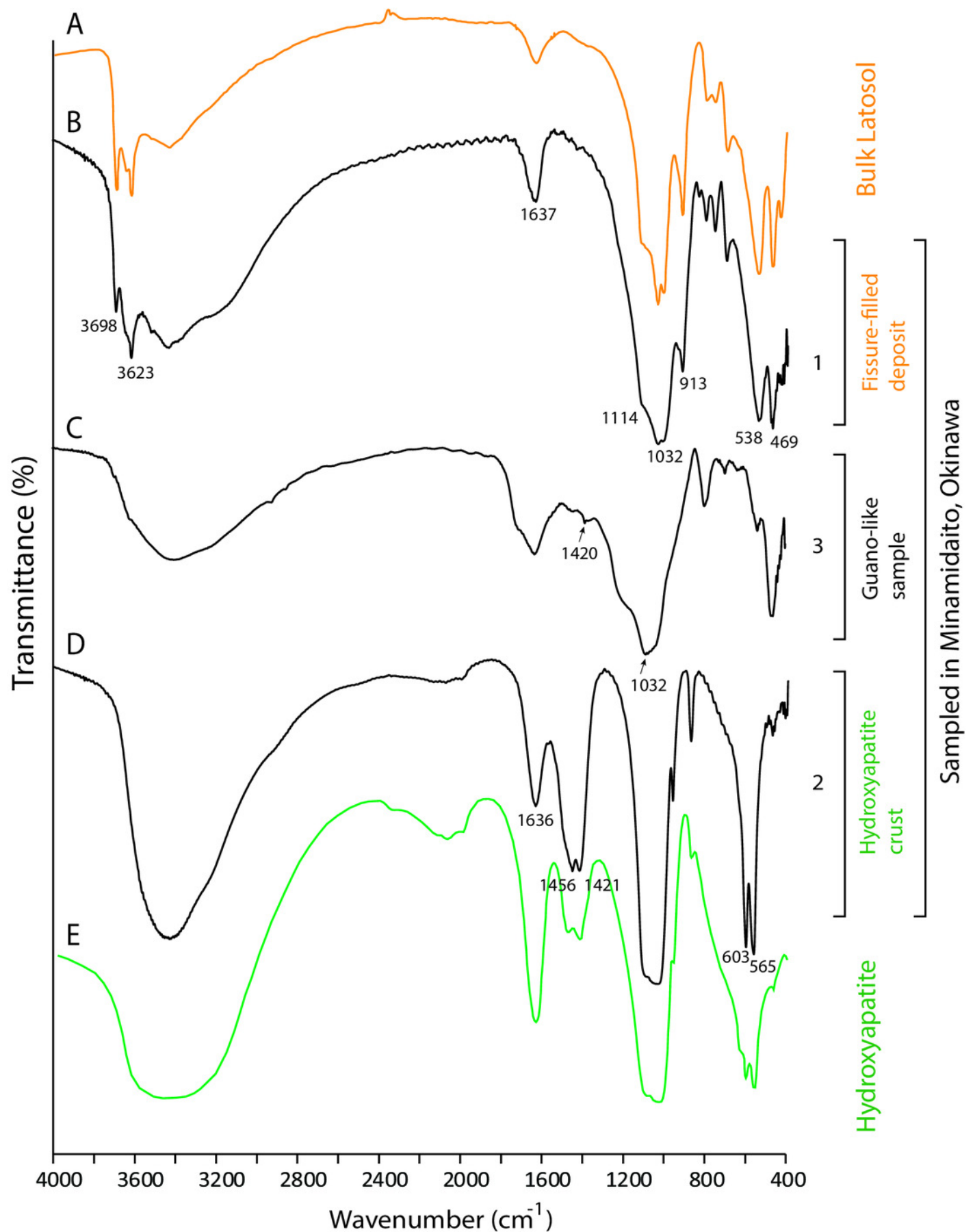
# Figure 8

Figure 8. Isotopic composition of carbon and nitrogen, total nitrogen by weight percent (%N), and C:N ratio in the selected guano-like samples and guano references, corresponding to Table 2.

(A) Stable nitrogen isotope values vs. %N; (B) Stable carbon isotope values vs. C:N. u: upper, m: middle, b: bottom. Raw data are provided in Table S1.
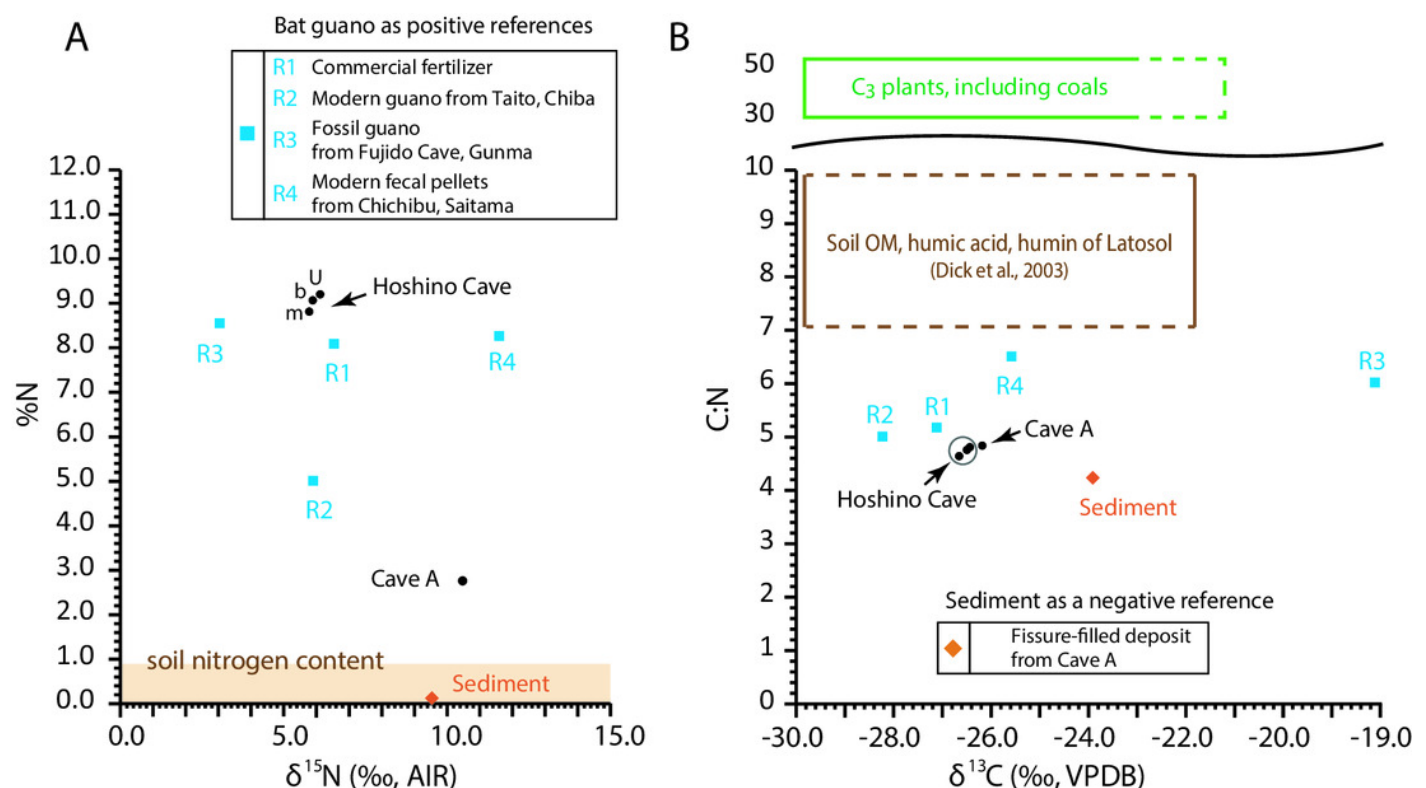
# Figure 9

Estimated δ¹³C values of vegetation based on bone apatite of cave-dwelling bats and chronological ranges of the extirpated bats on Minami-Daito Island.

(A) Estimated $\delta^{13}C$ values of vegetation on Minami-Daito Island, calculated from bone apatite

$\delta^{13}C$ values of the cave-dwelling bats. Measured $\delta^{13}C$ values of bone apatite are provided in

Table 3. For the isotopic enrichment factors and $\delta^{13}C$ values of pure $C_3$- and $C_4$-vegetation

applied in this study, see Supplementary Article S1 for details. (B) Estimated ages of the

extirpated Minami-Daito bats with lines of evidence revealed by this study. Thicker and

darker lines indicate the time range that is more strongly supported.
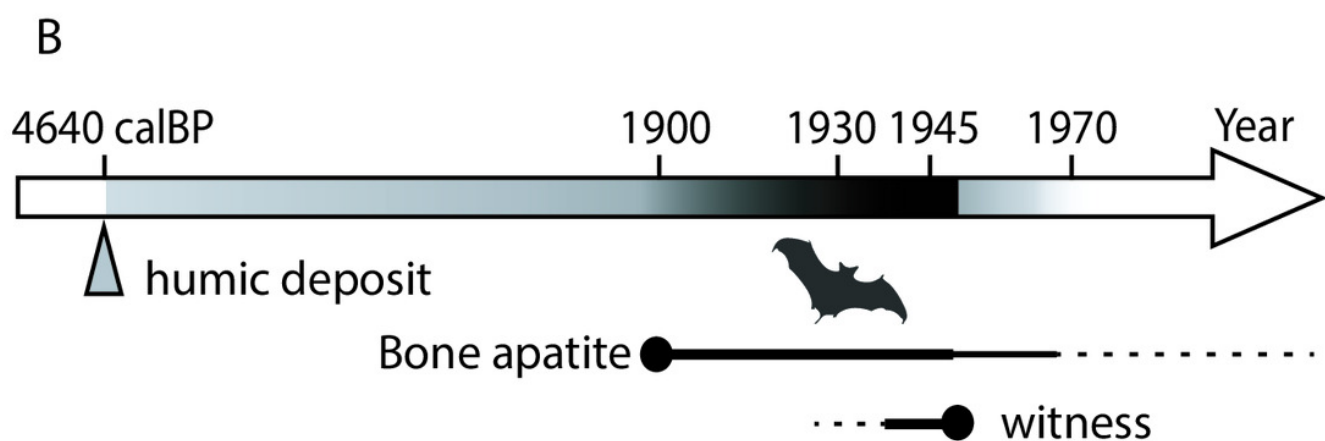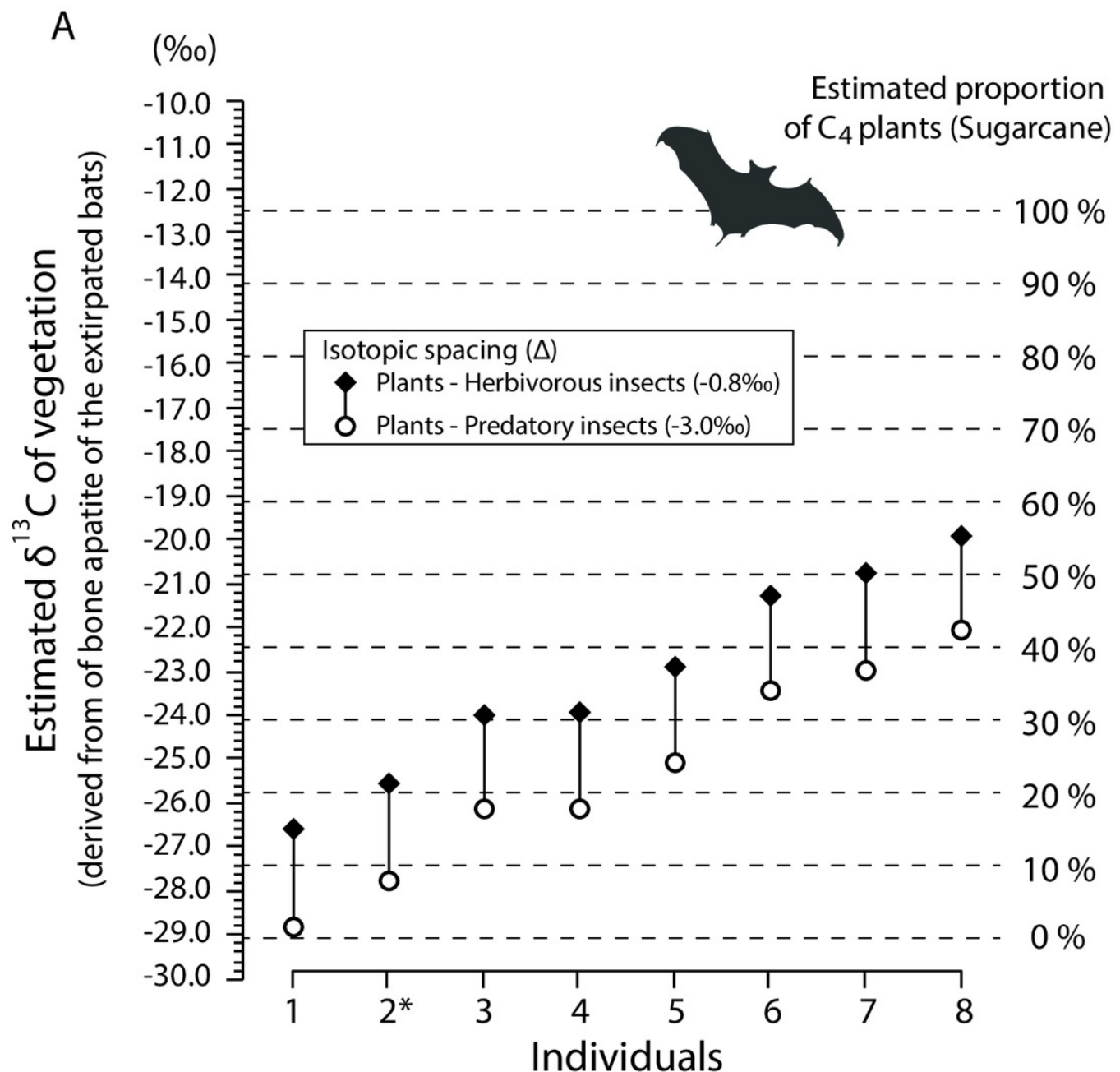
#Table 1**(on next page)**

Table 1. A list of skeletal remains of *Miniopterus* sp. and *Rhinolophus* sp. collected from Minami-Daito Island, Okinawa.

At the National Museum of Nature and Science (Tokyo, Japan), all vertebrate fossils

catalogued in the Department of Geology and Paleontology start with the prefix "NMNS-PV".

**Table 1**

| Museum ID (NMNS-PV) | NMNS-PV branch number | Scientific name | Estimated # of individual | Identification | Cave | Field Sampling ID |
|---|---|---|---|---|---|---|
| 23770 | | *Miniopterus* sp. | 1 | Articulated body | Cave A | NA |
| 23771 | | *Miniopterus* sp. | 1 | Articulated body | Cave A | NA |
| 23772 | 1 | *Rhinolophus* sp. | 1 | Left maxilla with two molars (partial) | Hoshino Cave | H160114-01-G |
| | 2 | | | Left mandible with teeth (m1-m3) | | H160114-01-A |
| | 3 | | | Right mandible without teeth (partial, fragmented) | | H160114-01-F |
| | 4 | | | Left radius (partial) | | H160114-01-C |
| | 5 | | | Radius? (partial) | | H160114-01-E |
| | 6, 7 | | | Pelvic bone (fragment), rib (partial), | | H160114-01-B |
| | 8 | | | Left humerus (almost complete) | | H160114-01-D |
| | NA | | | Skull (zygomatic arch only), bone fragments | | H160114-01-H |
| 23773 | 1 | *Rhinolophus* sp. | 1 | Left maxilla with teeth (partial) | Cave A | Y160113-10-C |
| | 2 | | | Left mandible (fragment) | | Y160113-10-G |
| | 3,4,5,6,7,8,9 | | | Right mandible with teeth (fragmented) | | Y160113-10-B |
| | 10 | | | Left clavicle (complete) | | Y160113-10-D |
| | 11 | | | Left radius (fragment) | | Y160113-10-H |
| | 12 | | | Radius? (fragment, small rod branched off), bone fragments | | Y160113-10-J |
| | 13 | | | Left humerus (partial) | | Y160113-10-I |
| | 14 | | | Pelvic bone (almost complete), bone fragment | | Y160113-10-A |
| | 15 | | | Metacarpal or phalange (partial)? | | Y160113-10-E |
| | 16 | | | Metacarpal? (partial) | | Y160113-10-K |
| | NA | | | Bone fragment (could not identified by YK) | | Y160113-10-F |

| | | | | | | |
|---|---|---|---|---|---|---|
| | NA | | | Bone fragments | | Y160113-10-L |
| 23774 | 1 | *Miniopterus* sp. | 1 | Left radius (fragment) | Cave A | Y160113-04-B |
| | 2 | | | Right radius (complete) | | Y160113-04-D |
| | 3 | | | Left humerus (fragment) | | Y160113-04-E |
| | 4 | | | Right humerus (complete) | | Y160113-04-C |
| | 5 | | | Metacarpal (fragment) | | Y160113-04-J |
| | 6,7 | | | Metacarpal or phalange? (fragments) | | Y160113-04-A |
| | NA | | | Bone fragments | | Y160113-04-G |
| 23775 | | *Miniopterus* sp. | 1 | Right radius (complete) | Cave A | Y160113-05-A |
| 23776 | | *Miniopterus* sp. | 1 | Right radius (almost complete) | Cave A | Y160113-06-A |
| 23777 | 1 | *Miniopterus* sp. | 1 | Skull | Cave A | Y160113-08-F |
| | 2 | | | Left radius (partial) | | Y160113-08-A |
| | 3 | | | Left humerus (complete) | | Y160113-08-E |
| | 4 | | | Right humerus (fragment) | | Y160113-08-D |
| | 5 | | | Metacarpal (fragment) | | Y160113-08-G |
| | NA | | | Bone fragments | | Y160113-08-B |
| 23778 | 1 | *Miniopterus* sp. | 1 | Skull (partial, fragment) without teeth | Cave A | Y160113-03-A |
| | 2,3,4,5,6,7,8 | | | Isolated teeth | | Y160113-03-B |
| | 9 | | | Right dentary wo teeth | | Y160113-03-K |
| | 10,11,12,13,14,15,16,18,19,20,21 | | | Left dentary, five islated teeth | | Y160113-03-I |
| | 22 | | | Isolated tympanic bulla (partial) | | Y160113-03-O |
| | 23,24 | | | Scapula (fragment), skull (zygomatic arch only) | | Y160113-03-N |
| | 25 | | | Right radius (fragment) | | Y160113-03-C |

| | 26 | | | Right humerus | | Y160113-03-H |
|---|---|---|---|---|---|---|
| | 27,28,29 | | | Metacarpal | | Y160113-03-E |
| | 30 | | | Metacarpal, metacarpal or phalange? (fragments) | | Y160113-03-F |
| | 31 | | | Metacarpal (fragment) | | Y160113-03-J |
| | 32 | | | Metacarpal or phalange? (fragment) | | Y160113-03-M |
| | 33,34,35,36 | | | Rib | | Y160113-03-D |
| | NA | | | Bone fragment (radius, left or right unidentified) | | Y160113-03-G |
| | NA | | | Bone fragment (radius, left or right unidentified) | | Y160113-03-L |
| | NA | | | Bone fragments | | Y160113-03-P |
| 23779 | 1 | *Miniopterus* sp. | 1 | Skull (maxilla with ful dentition, others fragmented) | Cave A | Y160114-01-A |
| | 2 | | | Right mandible with dentition (almost complete) | | Y160114-01-G |
| | 3 | | | Isolated antemolar | | Y160114-01-G |
| | 4 | | | Atlas (complete) | | Y160114-01-E |
| | 5 | | | Left radius (fragment) | | Y160114-01-C |
| | 6 | | | Right radius (almost complete) | | Y160114-01-F |
| | 7 | | | Left humerus (complete) | | Y160114-01-B |
| | 8 | | | Right humerus (complete) | | Y160114-01-D |
| | 9 | | | Left femur (complete) | | Y160114-01-H |
| | NA | | | Bone fragments | | Y160114-01-I |
| 23780 | 1 | *Miniopterus* sp. | 1 | Skull | Cave A | Y160114-02-A |
| | 2 | | | Left mandible | | Y160114-02-D |
| | 3,4,5 | | | Axis, cervical bones | | Y160114-02-F |
| | 6 | | | Thoracic vertebrate (partial) | | Y160114-02-J |

| | | | | | |
|---|---|---|---|---|---|
| | 7 | | | Clavicle (complete) | Y160114-02-I |
| | 8 | | | Left scapula (partial) | Y160114-02-G |
| | 9 | | | Left radius (complete) | Y160114-02-H |
| | 10 | | | Left humerus (fused with other bones by calcite crystals) | Y160114-02-E |
| | 11 | | | Right humerus (partial) | Y160114-02-B |
| | 12,13 | | | Metacarpals (partial) | Y160114-02-C |
| | 14,15,16,17,18,19,20 | | | Ribs | Y160114-02-K |
| | NA | | | Metacarpals or carpal (fragment) | Y160114-02-M |
| | NA | | | Bone fragment | Y160114-02-L |
| 23781 | 1 | *Miniopterus* sp. | 1 | Skull (partial), skull fragments | Y160114-03-A |
| | 2,3,4,5,6,7 | | | temparate bullae, isolated teeth | Y160114-03-I |
| | 8 | | | Left radius (complete) | Y160114-03-C |
| | 9 | | | Right radius (complete) | Y160114-03-B |
| | 10 | | | Left humerus (fragment) | Y160114-03-H |
| | 11 | | | Right humerus (complete) | Y160114-03-G |
| | 12 | | | Right femur | Y160114-03-E |
| | 13 | | | Metacarpal (partial) | Y160114-03-D |
| | 14 | | | Metacarpal (partial) | Y160114-03-J |
| | 15 | | | Metacarpal (partial) | Y160114-03-K |
| | 16 | | | Metacarpal (partial) | Y160114-03-L |
| | NA | | | Metacarpal (fragment) | Y160114-03-F |
| 23782 | 1 | *Miniopterus* sp. | 1 | Left maxila with dentition (partial) | Y160114-04-E |
| | 2,3 | | | Left dentary with dentition (complete), isolated m1 (trigonid basin only) | Y160114-04-C |
| | 4,5 | | | Right dentary with dentition (complete), isolated antemolar | Y160114-04-D |

Note: The "Cave A" location label spans the rows for specimens 23781 and 23782.

| | | | | | Right radius (partial) | | Y160114-04-B |
|---|---|---|---|---|---|---|---|
| | 6 | | | | Right radius (partial) | | Y160114-04-B |
| | NA | | | | Metacarpal or phalange (fragments) | | Y160114-04-A |
| | NA | | | | Bone fragments | | Y160114-04-F |
| 23783 | 1 | *Miniopterus* sp. | 2 | | Left radius (partial) | Cave A | Y160113-07-B |
| | 2 | | | | Left? radius (fragment) | | Y160113-07-D |
| | 3 | | | | Right radius (complete) | | Y160113-07-E |
| | 4 | | | | Right? radius (fragment) | | Y160113-07-K |
| | 5 | | | | Left humerus (complete) | | Y160113-07-F |
| | 6 | | | | Left humerus (complete) | | Y160113-07-A |
| | 7 | | | | Right humerus (complete) | | Y160113-07-G |
| | 8 | | | | Right humerus, bone fragment | | Y160113-07-C |
| | NA | | | | Metacarpal or phalange? (bone fragments) | | Y160113-07-H |
| 23784 | | *Miniopterus* sp. | 1 | | Left and right mandibles (complete, separated) | Cave A | |
| 23785 | | *Miniopterus* sp. | 1 | | Right maxilla with dentition (partial) | Cave A | |
| 24999 | | *Miniopterus* sp. | 1 | | Left mandible (partial) | Cave A | |
| 25000 | | *Miniopterus* sp. | 1 | | Right mandible (partial) | Cave A | |

Table 2. Summary of carbon and nitrogen isotopes, C:N ratios, weight percent of carbon and nitrogen in samples.

1   Table 2

| Sample ID | Material Type | Sampling locality | N | δC (‰, VPDB) | | δN (‰, AIR) | | C/N | | %C in sample | | %N in sample | |
|---|---|---|---|---|---|---|---|---|---|---|---|---|---|
| | | | | Average | SD | Average | SD | Average | SD | Average | SD | Average | SD |
| R1 | Modern guano (R1) | Commercial fertilizer | 5 | -27.1 | 0.22 | 6.5 | 0.37 | 5.2 | 0.24 | 41.8 | 1.0 | 8.1 | 0.5 |
| R2 | Modern guano (R2) | Taito, Chiba | 1 | -28.2 | | 5.9 | | 5.0 | | 44.8 | | 8.9 | |
| R3 | Modern fecal pellet (R3) | Chichibu, Saitama | 3 | -19.1 | 0.03 | 3.0 | 0.10 | 6.0 | 0.02 | 51.1 | 0.4 | 8.6 | 0.1 |
| R4 | Fossil guano (R4) | Fujido Cave, Ueno, Gunma | 1 | -25.6 | | 11.6 | | 6.5 | | 53.8 | | 8.3 | |
| Sediment | Fissure-filled cave deposit | #1 in Cave A | 7 | -23.9 | 0.15 | 9.5 | 0.17 | 4.2 | 0.24 | 0.5 | 0.03 | 0.1 | 0.002 |
| Y180119g2 | Fecal pellet-like sample | #3 in Cave A | 1 | -26.1 | | 10.2 | | 4.8 | | 13.2 | | 2.7 | |
| H180120g5-u | Guano-like deposit | #6 in Hoshino Cave | 1 | -26.4 | | 6.1 | | 4.8 | | 44.3 | | 9.2 | |
| H180120g5-m | Guano-like deposit | #6 in Hoshino Cave | 1 | -26.7 | | 5.8 | | 4.6 | | 40.9 | | 8.8 | |
| H180120g5-b | Guano-like deposit | #6 in Hoshino Cave | 1 | -26.5 | | 5.9 | | 4.8 | | 43.2 | | 9.1 | |

Stable carbon isotope values of bone apatite in the Minami-Daito cave-dwelling bats.

1    Table 3

| Individual # | Element | $\delta^{13}C$ (‰, VPDB) | Lab Code |
|---|---|---|---|
| 1 | Proximal end of right humerus | -15.0 | Y160113b−6 |
| 2 | Multiple bone fragments | -14.0 | Y160113b−201902−4−2 |
| 3 | Distal end of right humerus | -12.4 | Y160113b−8 |
| 4 | Left radius | -12.3 | Y160113b-201902-1 |
| 5 | Right radius | -11.3 | Y160113b−201902−2−2 |
| 6 | Distal end of humerus | -9.6 | Y160113b−5 |
| 7 | Proximal end of femur | -9.1 | Y160113b−7 |
| 8 | Fragments of left humerus and left radius | -8.3 | Y160113b−201902−3−2 |